A METHOD OF JET-WING INTERACTION NOISE PREDICTION AT LOW FREQUENCIES

Oleg Bychkov[1,2], **Georgy Faranosov[1]**

[1]Central Aerohydrodynamic Institute (TsAGI), Russia
[2]Moscow Institute of Physics and Technology (MIPT), Russia

RUSSIAN FOUNDATION FOR BASIC RESEARCH
Project 16-01-00746a

MINPROMTORG RUSSIA
Project ORINOCO-2

ARTEM
Horizon 2020

Outline

- Introduction
- Analytical model description
- Examples of application of the model
  - Jet-plate config. - comparison with experiments
  - Jet-plate config. - comparison with CAA results
  - Jet-wing-flap config. - comparison with experiments
- Conclusion

Outline

- Introduction
- Analytical model description
- Examples of application of the model

  - Jet-plate config. - comparison with experiments

  - Jet-plate config. - comparison with CAA results

  - Jet-wing-flap config. - comparison with experiments

- Conclusion

Motivation

Source: www.irkut.com

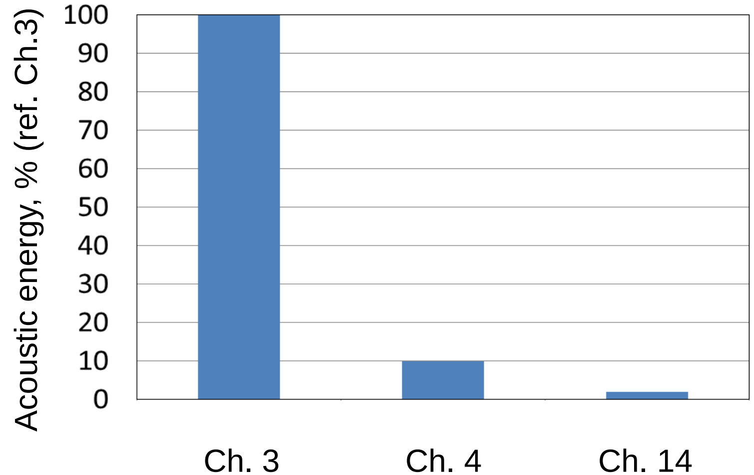

Short to medium range aircraft, BPR 10-12, approach

Source: www.fantassy.nlr.nl

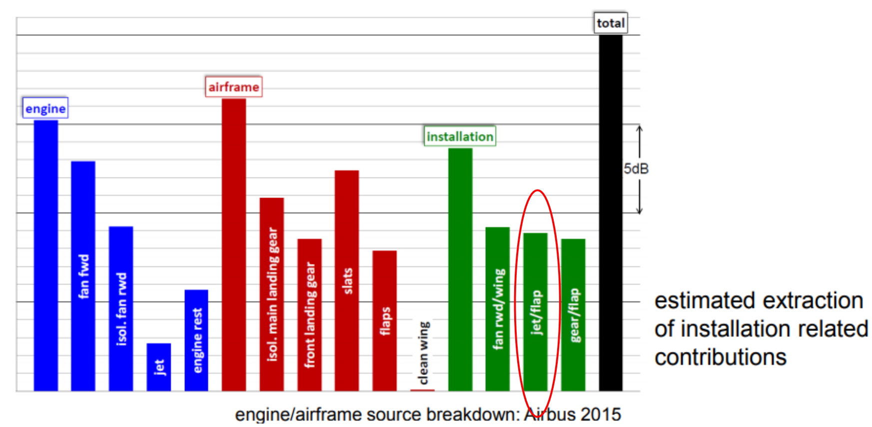

http://ceaa.imamod.ru/2016/files/ceaa2016.pdfs/D3S01_Delfs.pdf

Background

- Observer

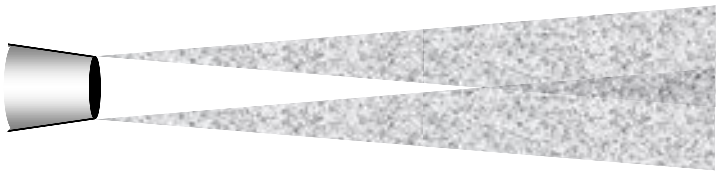

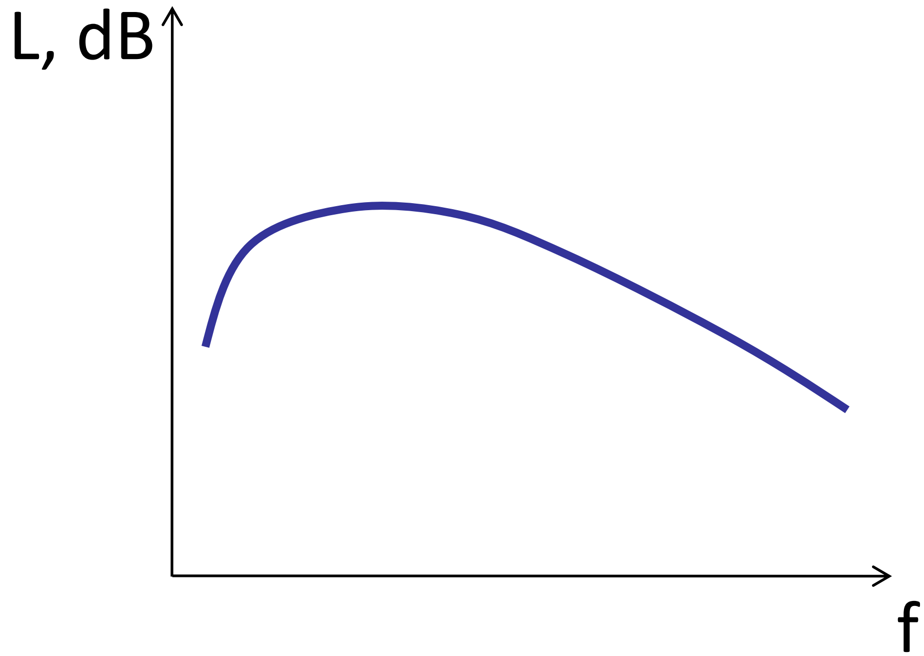

- Observer

Background

- Observer (shielded)

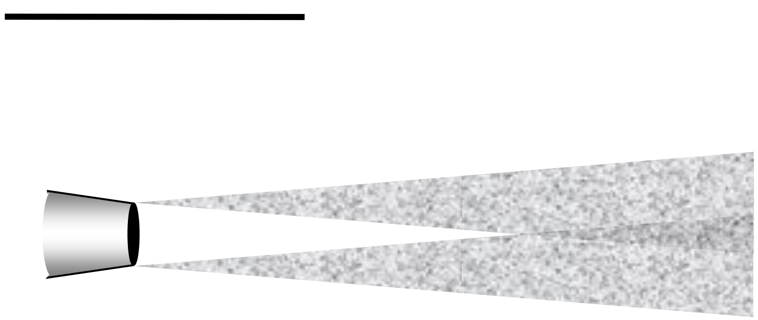

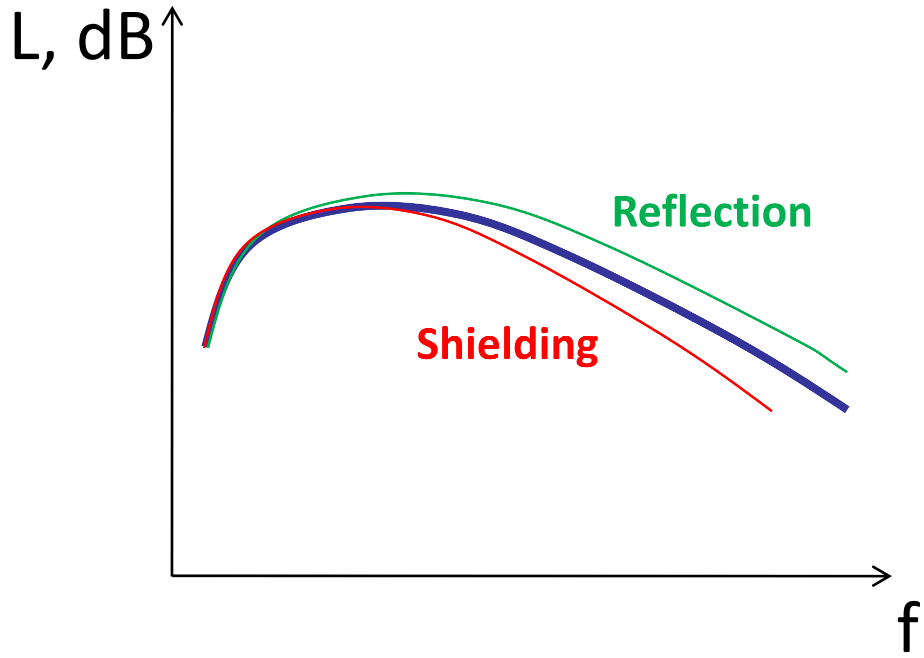

- Observer (unshielded)

Background

- Observer (shielded)

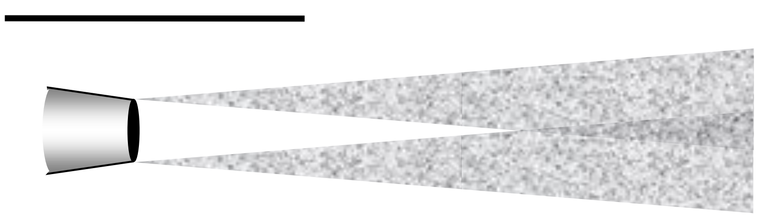

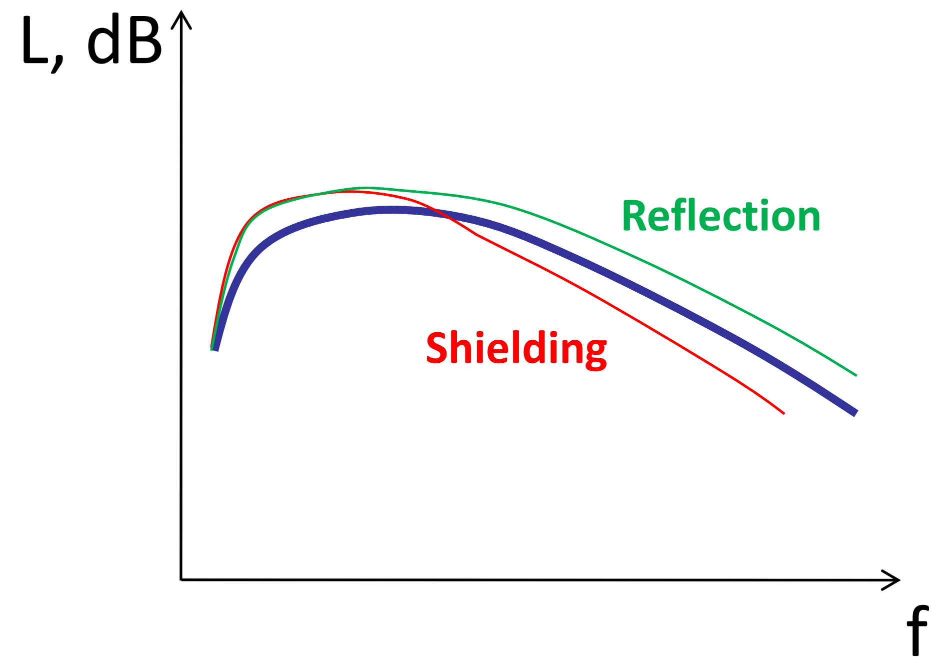

- Observer (unshielded)

Background

- Observer (shielded)

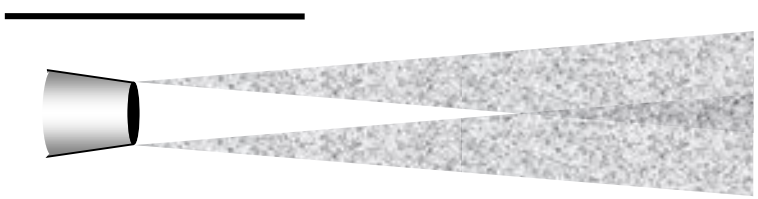

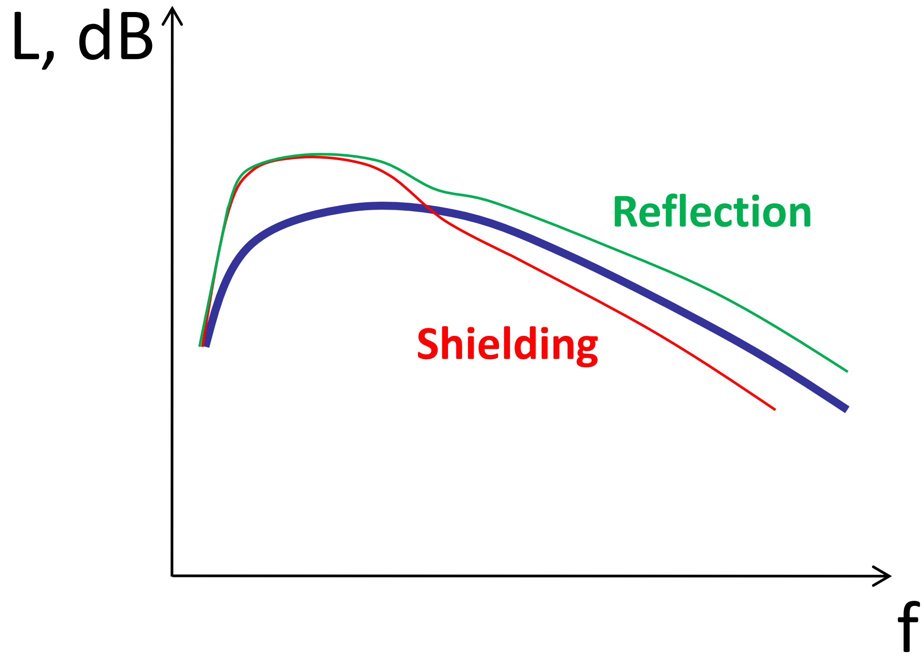

- Observer (unshielded)

Background

- Observer (shielded)

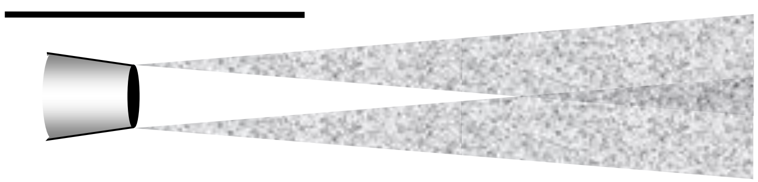

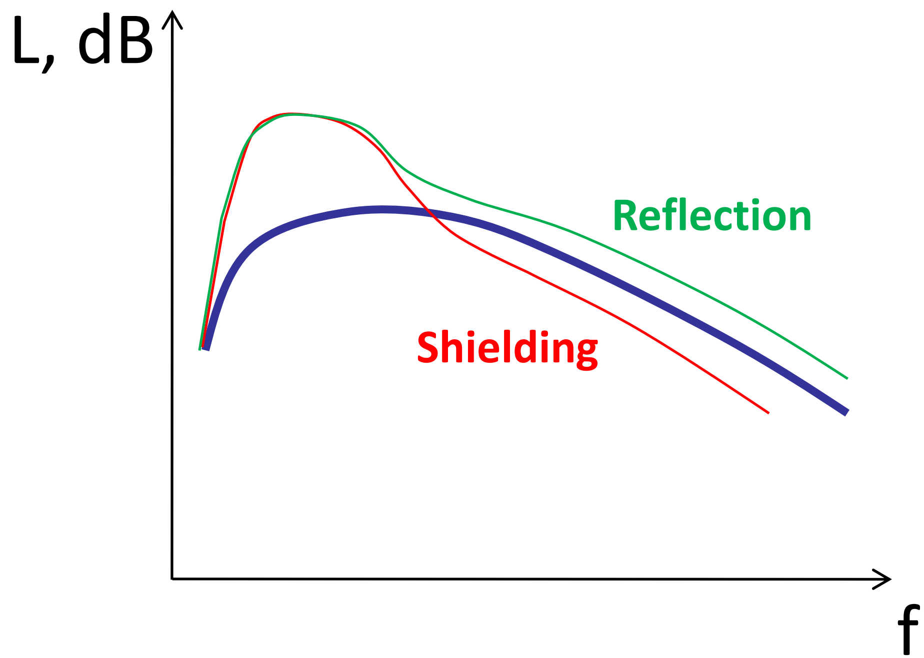

Broadbent (1977)

- Observer (unshielded)

Background

- Observer (shielded)

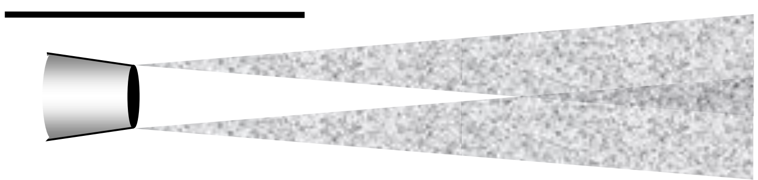

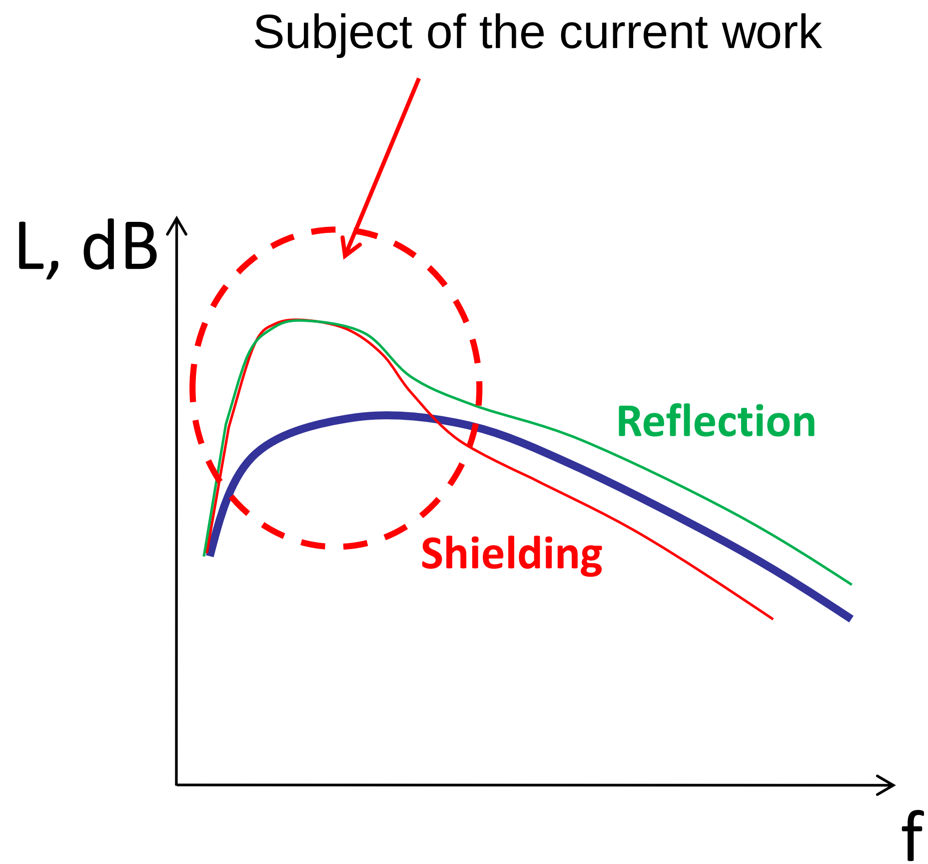

- Observer (unshielded)

Broadbent (1977)

Background

- **Observer (shielded)**

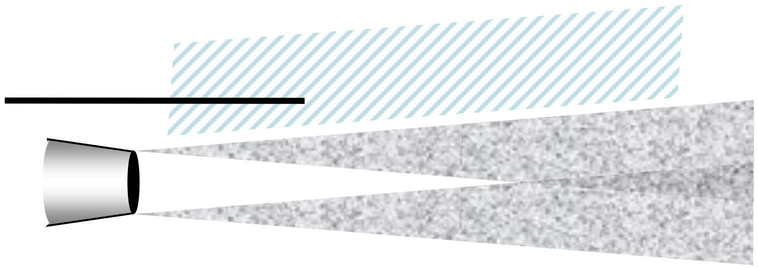

- **Observer (unshielded)**

Self et al. (2011)
Kopiev et al. (2013)
Faranosov&Bychkov (2014, 2016)
Jordan et al. (2012, 2014, 2016)
Dowling et al. (2016-2018)
Faranosov et al. (2016-2018)

Background

- **Observer (shielded)**

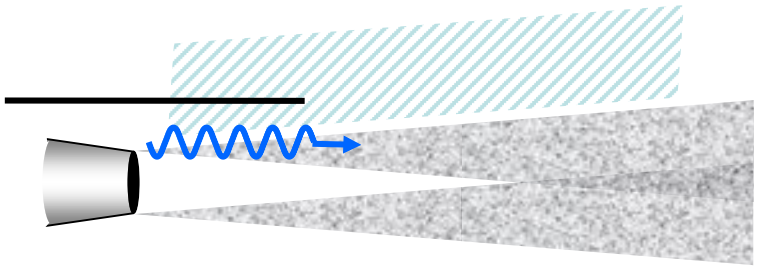

Self et al. (2011)
Kopiev et al. (2013)
Faranosov&Bychkov (2014, 2016)
Jordan et al. (2012, 2014, 2016)
Dowling et al. (2016-2018)
Faranosov et al. (2016-2018)

1. **Modeling of pulsations properties**

- **Observer (unshielded)**

Background

- Observer (shielded)

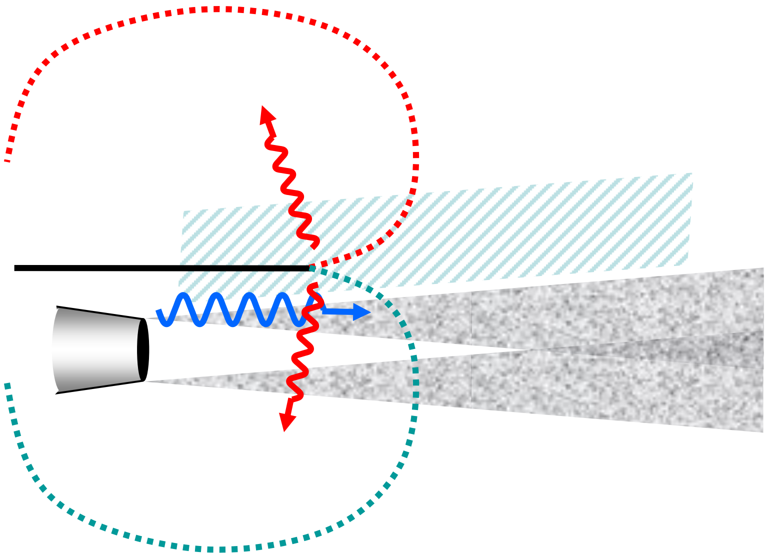

- Observer (unshielded)

Self et al. (2011)
Kopiev et al. (2013)
Faranosov&Bychkov (2014, 2016)
Jordan et al. (2012, 2014, 2016)
Dowling et al. (2016-2018)
Faranosov et al. (2016-2018)

1. **Modeling of pulsations properties**
2. **Solution of the diffraction problem**

Ffowcs Williams&Hall (1970)
Amiet (1976)

Background

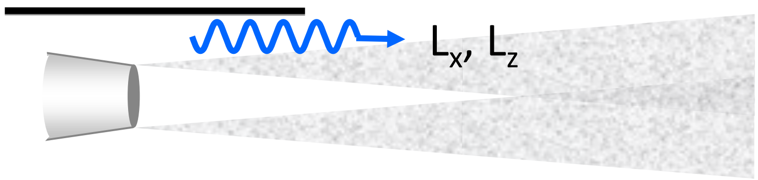

Self et al. (2011)
Kopiev et al. (2013)
Faranosov&Bychkov (2014, 2016)
Jordan et al. (2012, 2014, 2016)
Dowling et al. (2016-2018)
Faranosov et al. (2016-2018)

1. **Modeling of pulsations properties**
2. **Solution of the diffraction problem**

Ffowcs Williams&Hall (1970)
Amiet (1976)

Background

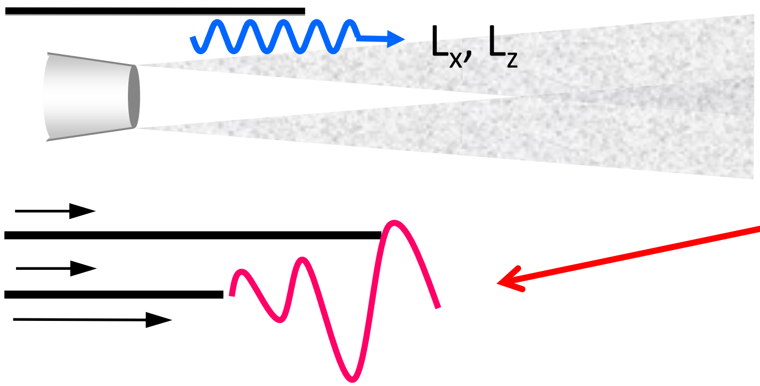

Self et al. (2011)
Kopiev et al. (2013)
Faranosov&Bychkov (2014, 2016)
Jordan et al. (2012, 2014, 2016)
Dowling et al. (2016-2018)
Faranosov et al. (2016-2018)

1. **Modeling of pulsations properties**
2. **Solution of the diffraction problem**

Ffowcs Williams&Hall (1970)
Amiet (1976)

Background

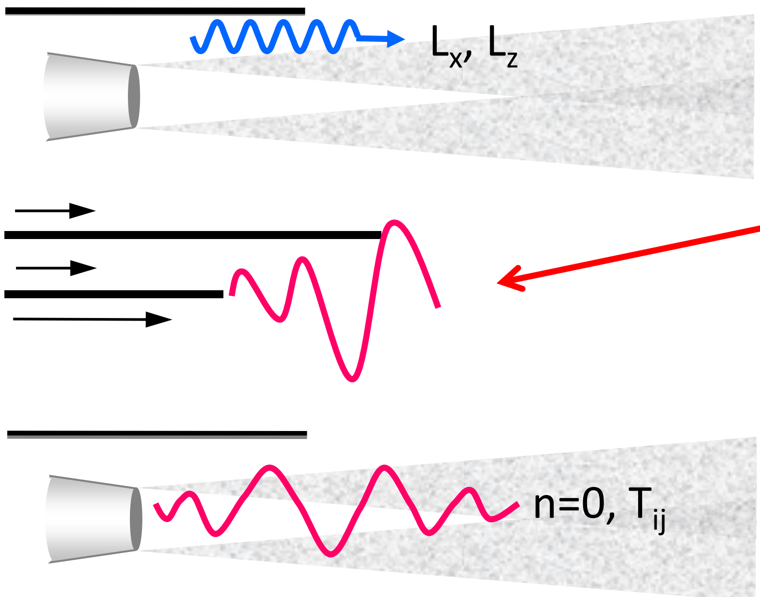

Self et al. (2011)
Kopiev et al. (2013)
Faranosov&Bychkov (2014, 2016)
Jordan et al. (2012, 2014, 2016)
Dowling et al. (2016-2018)
Faranosov et al. (2016-2018)

1. **Modeling of pulsations properties**
2. **Solution of the diffraction problem**

Ffowcs Williams&Hall (1970)
Amiet (1976)

Background

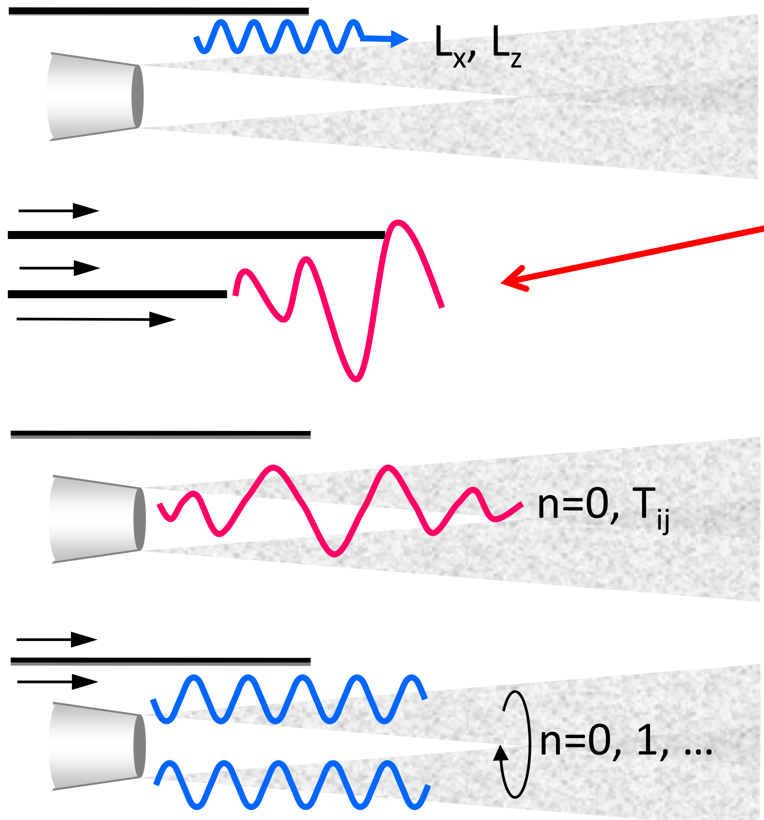

Self et al. (2011)
Kopiev et al. (2013)
Faranosov&Bychkov (2014, 2016)
Jordan et al. (2012, 2014, 2016)
Dowling et al. (2016-2018)
Faranosov et al. (2016-2018)

1. **Modeling of pulsations properties**
2. **Solution of the diffraction problem**

Ffowcs Williams&Hall (1970)
Amiet (1976)

Background

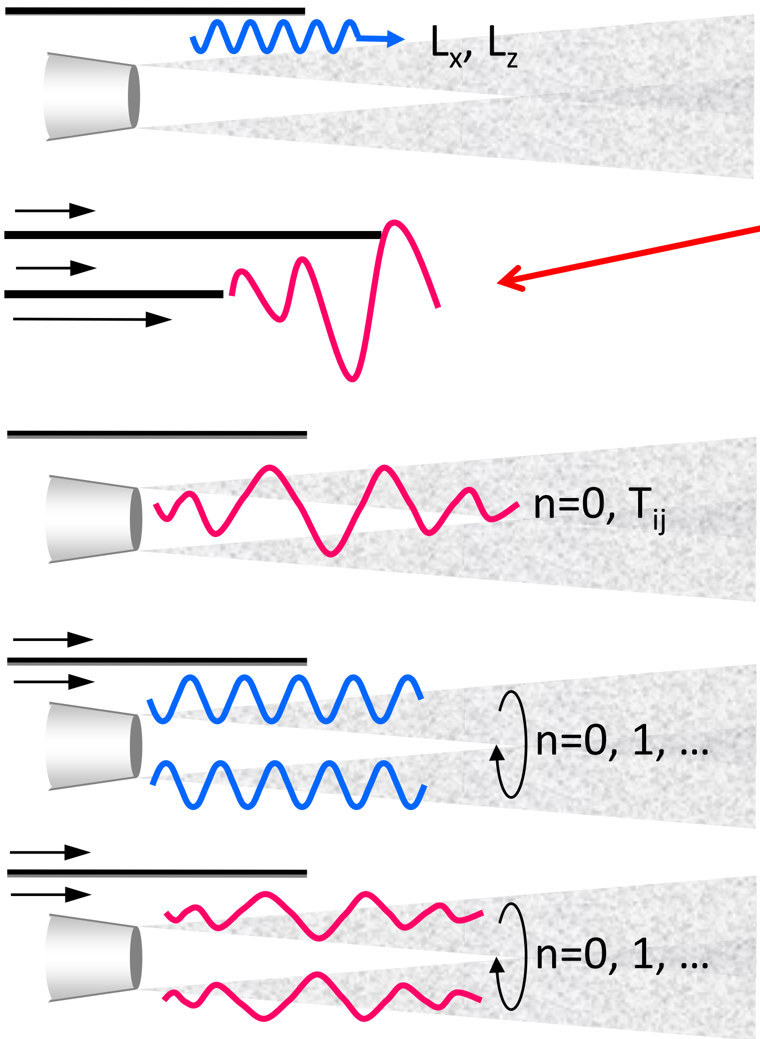

Self et al. (2011)
Kopiev et al. (2013)
Faranosov&Bychkov (2014, 2016)
Jordan et al. (2012, 2014, 2016)
Dowling et al. (2016-2018)
Faranosov et al. (2016-2018)

1. **Modeling of pulsations properties**
2. **Solution of the diffraction problem**

Ffowcs Williams&Hall (1970)
Amiet (1976)

Outline

- Introduction
- Analytical model description
- Examples of application of the model
  - Jet-plate config. - comparison with experiments
  - Jet-plate config. - comparison with CAA results
  - Jet-wing-flap config. - comparison with experiments
- Conclusion

Installation noise modeling

Near-field pulsations are represented as Gaussian wavepackets – incident field for the diffraction problem

$$p_i(r,x,\theta) \approx \sum_{n=-\infty}^{\infty} \frac{A_n}{\delta_n\sqrt{\pi}} \frac{K_n(\beta_n r)}{K_n(\beta_n r_0)} e^{in\theta - \frac{(x-x_{0n})^2}{\delta_n^2} + i\omega\frac{x-x_{0n}}{V_{cn}}}.$$

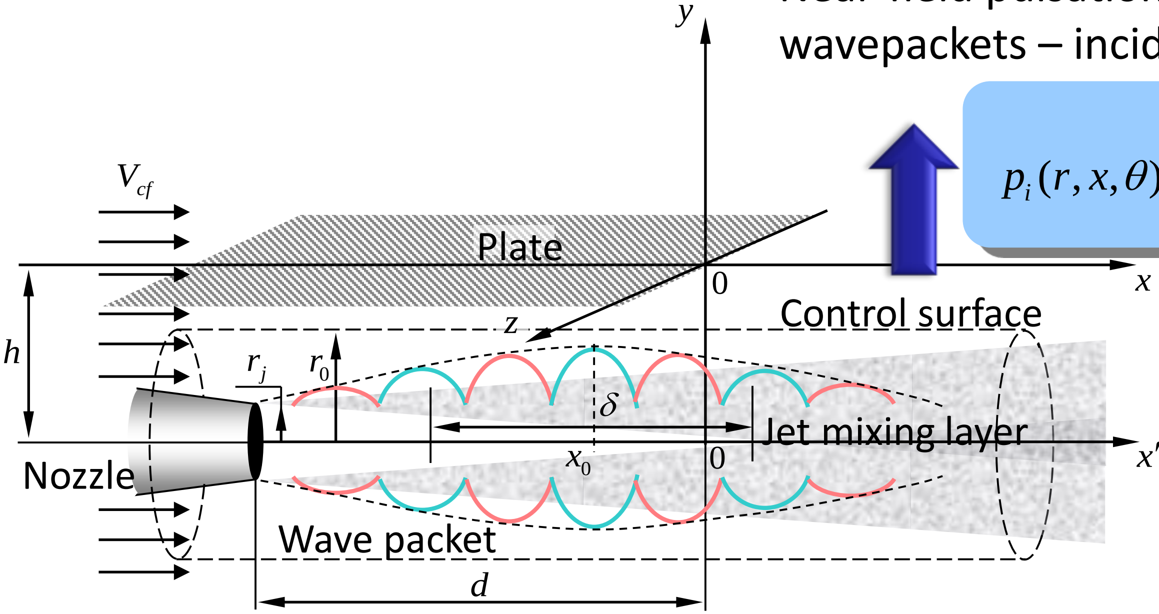

Installation noise modeling

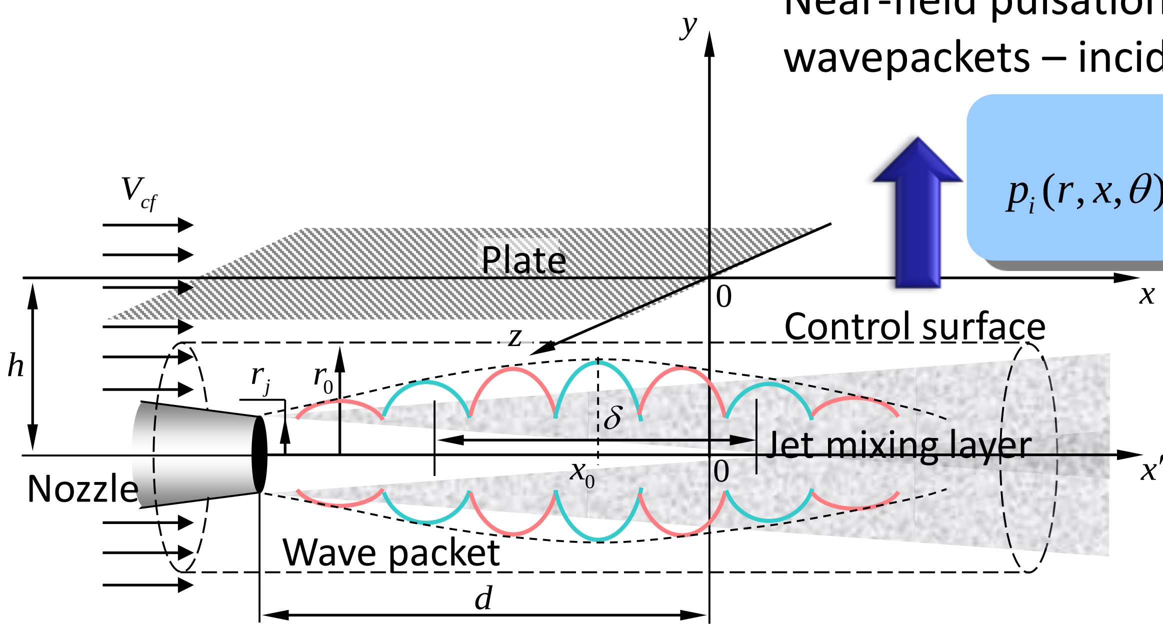

Near-field pulsations are represented as Gaussian wavepackets – incident field for the diffraction problem

$$p_i(r,x,\theta) \approx \sum_{n=-\infty}^{\infty} \frac{A_n}{\delta_n\sqrt{\pi}} \frac{K_n(\beta_n r)}{K_n(\beta_n r_0)} e^{in\theta - \frac{(x-x_{0n})^2}{\delta_n^2} + i\omega\frac{x-x_{0n}}{V_{cn}}}.$$

1. Wiener-Hopf teqnique
2. 2D steepest descent method

Far-field sound – contribution from each azimuthal mode

$$|p_n(r,\chi)| \approx \hat{A}_n \left| \frac{\sin(\chi/2)}{\alpha_{sn}\frac{M_n}{k} + M_n\cos\chi} \right|, \quad \hat{A}_n = A_n \frac{M_n}{\sqrt{2\pi k\delta_n r}} \left| \frac{e^{-\frac{(d-x_{0n})^2}{\delta_n^2} - \beta_{cf}(\alpha_{sn})h}}{K_n\left(\beta_{cf}(\alpha_{sn})r_0\right)\beta_{cf+}(\alpha_{sn})} \right|.$$

A_n, δ_n, M_n – can be taken from experiments or numerical simulation

Outline

- Introduction
- Analytical model description
- Examples of application of the model
  - Jet-plate config. - comparison with experiments
  - Jet-plate config. - comparison with CAA results
  - Jet-wing-flap config. - comparison with experiments
- Conclusion

Test rig

TsAGI anechoic chamber AC-2

Single-stream round jet, D=40 mm

Wing is simulated by a rectangular plate 1.2m x 0.35m x 0.003m

Installation parameters:
h = D, d = 3.2 D (the edge in the linear hydrodynamic field)

M_j = 0.4, 0.53, 0.6, 0.7, 0.82, 0.88

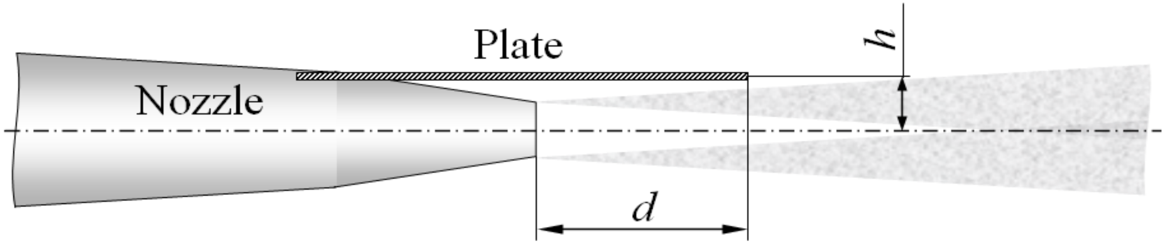

Far-field acoustic measurements were conducted by an azimuthal array

(Faranosov et al. 2017)

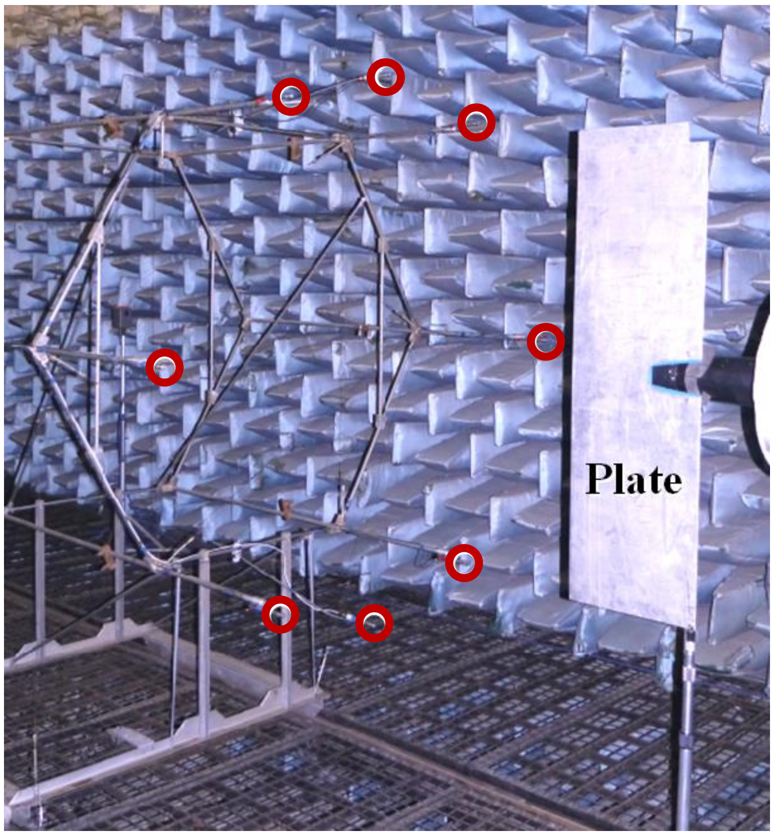

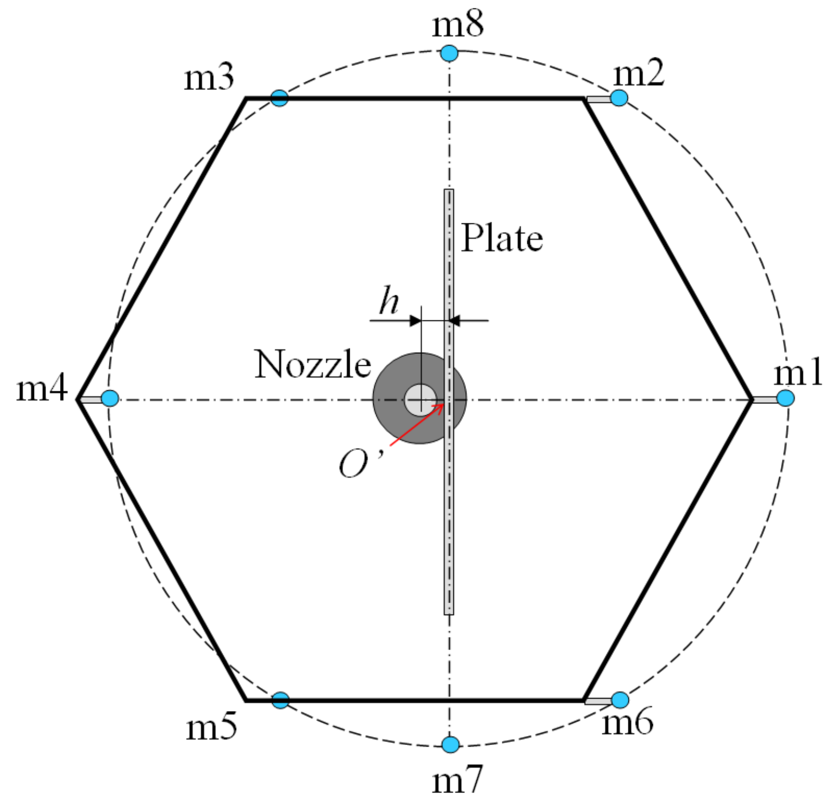

Far-field acoustic measurements

M_j=0.4

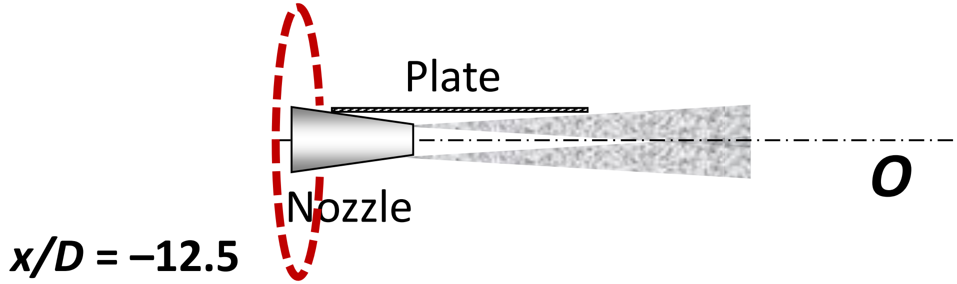

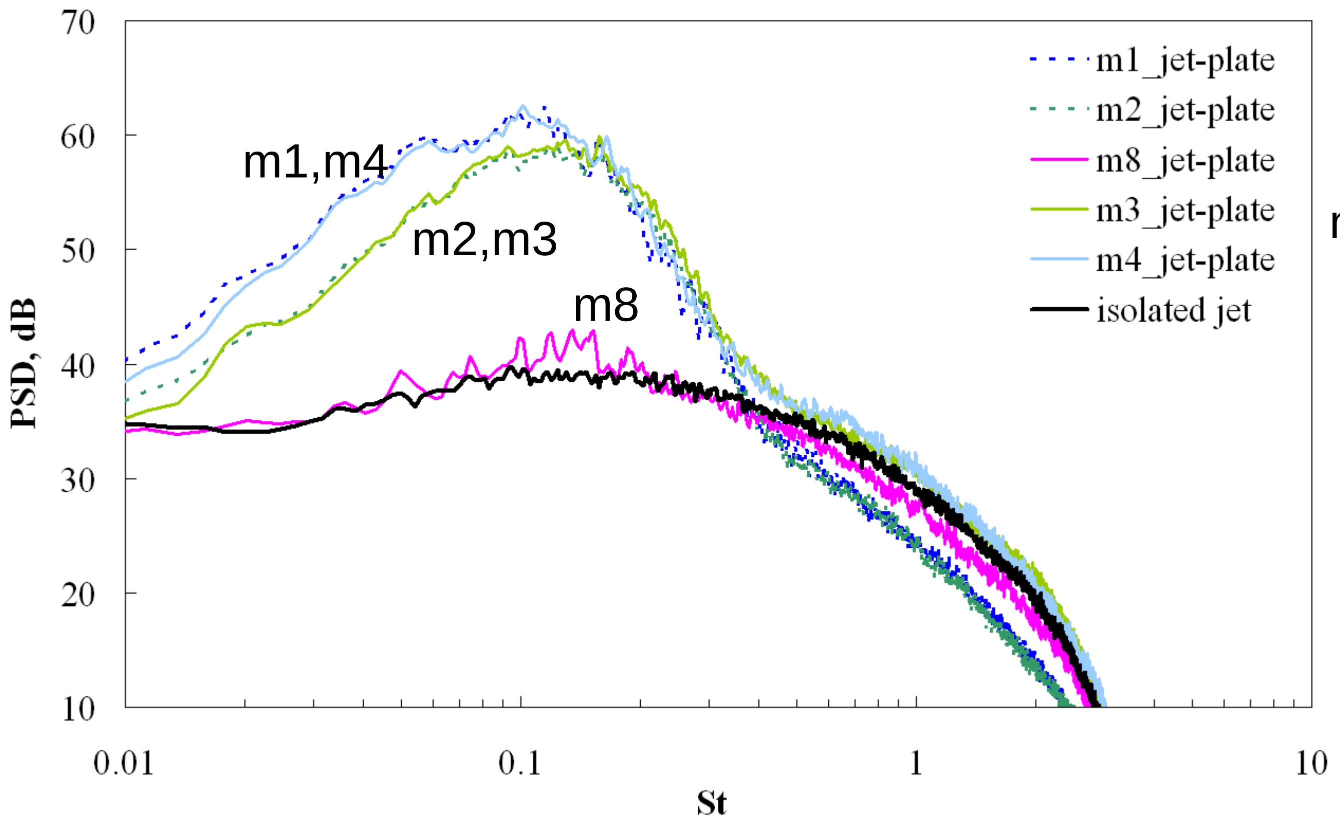

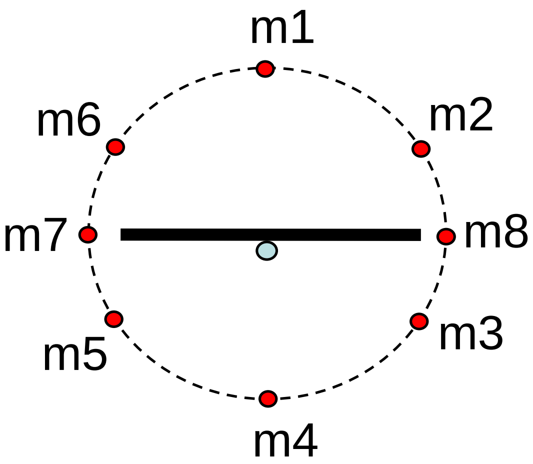

Far-field acoustic measurements

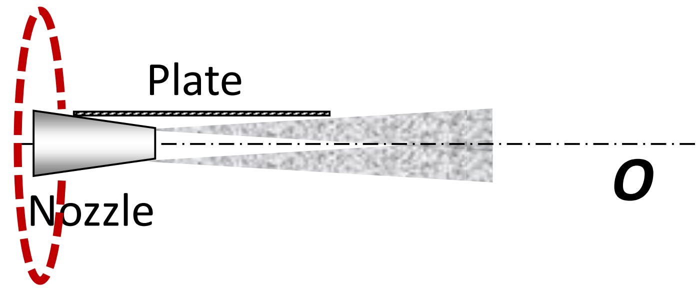

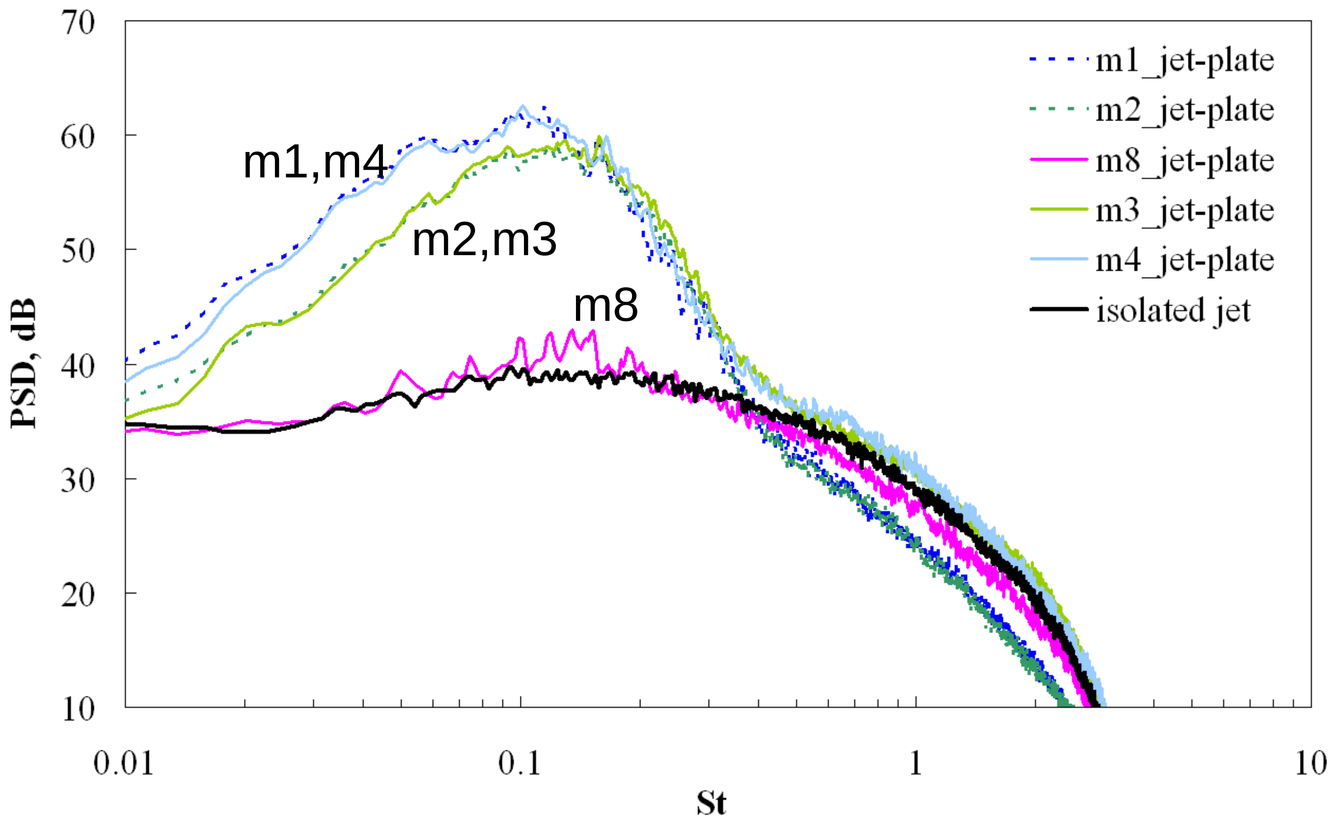

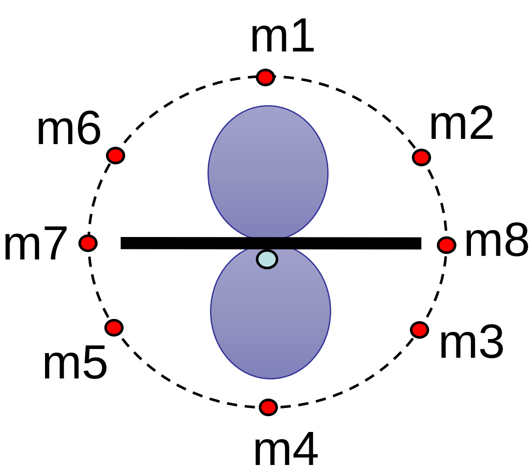

Far-field acoustic measurements

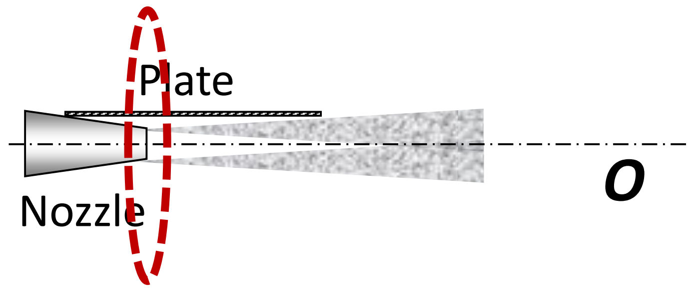

M_j=0.4

***x/D* = 0**

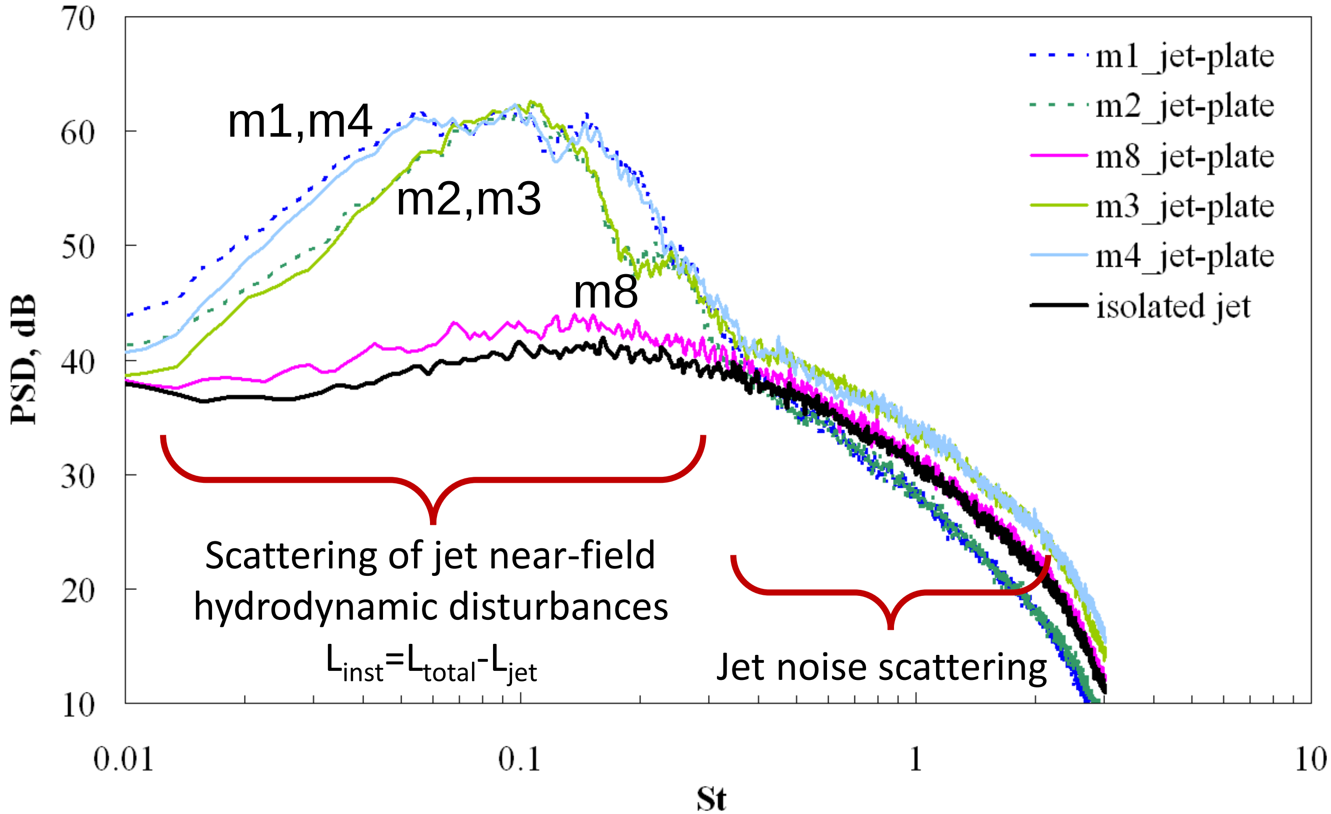

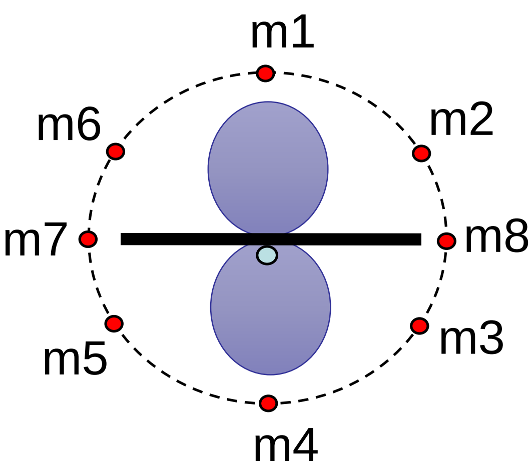

Kopiev et al. 2013
Jordan et al. 2013
Bychkov et al. 2016
Lyu&Dowling 2017

Far-field acoustic measurements

M_j=0.4

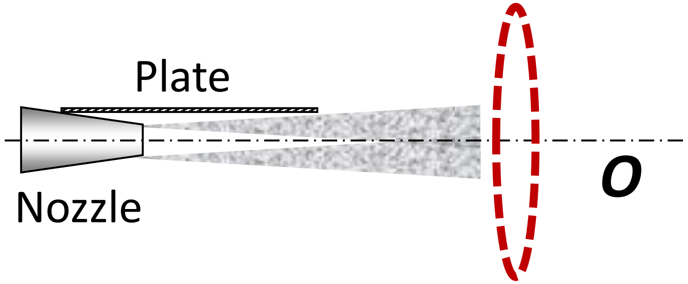

x/D =38

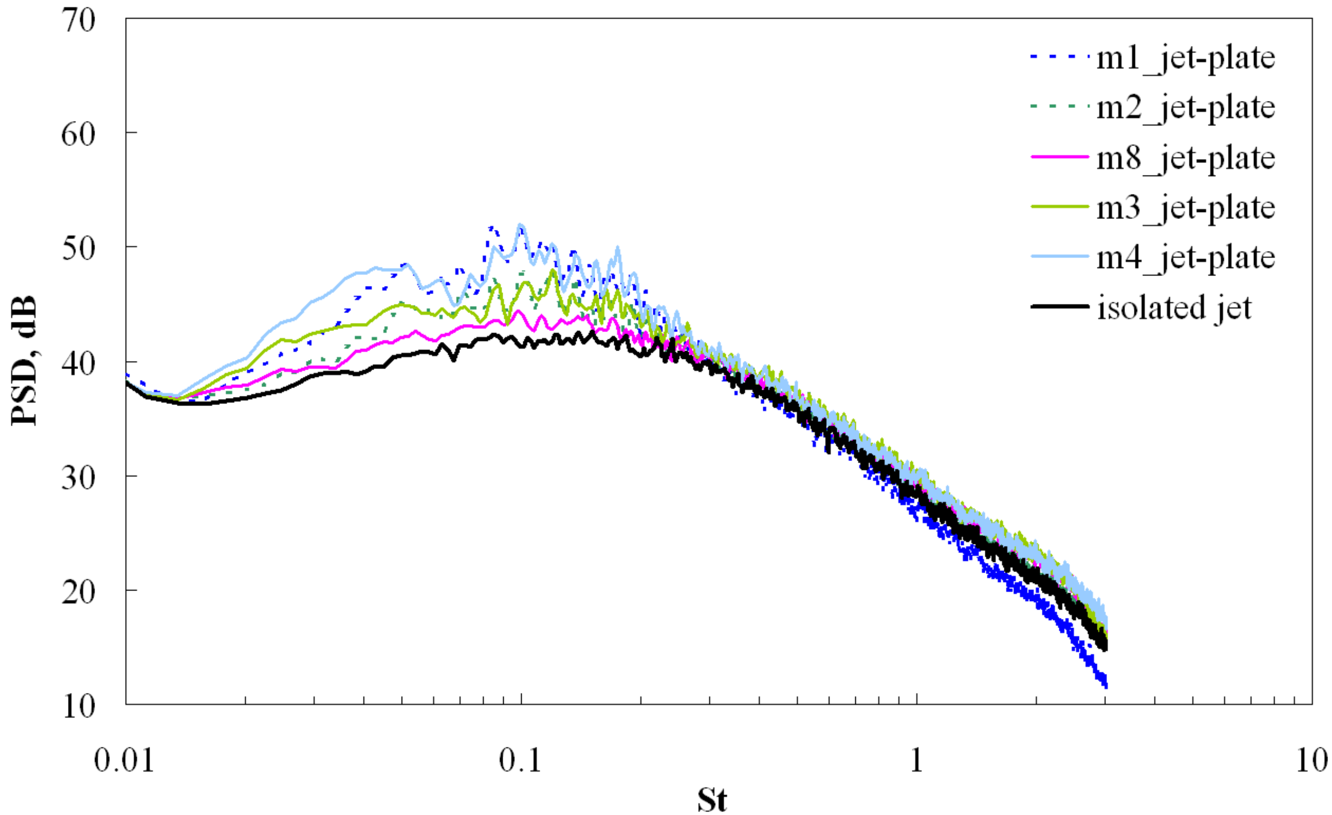

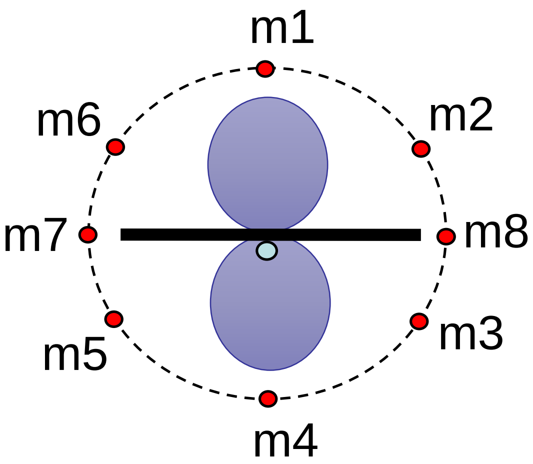

Experimental investigation of the near-field structure

Detailed description of the experiment may be found in *Kopiev et al. (2017)*

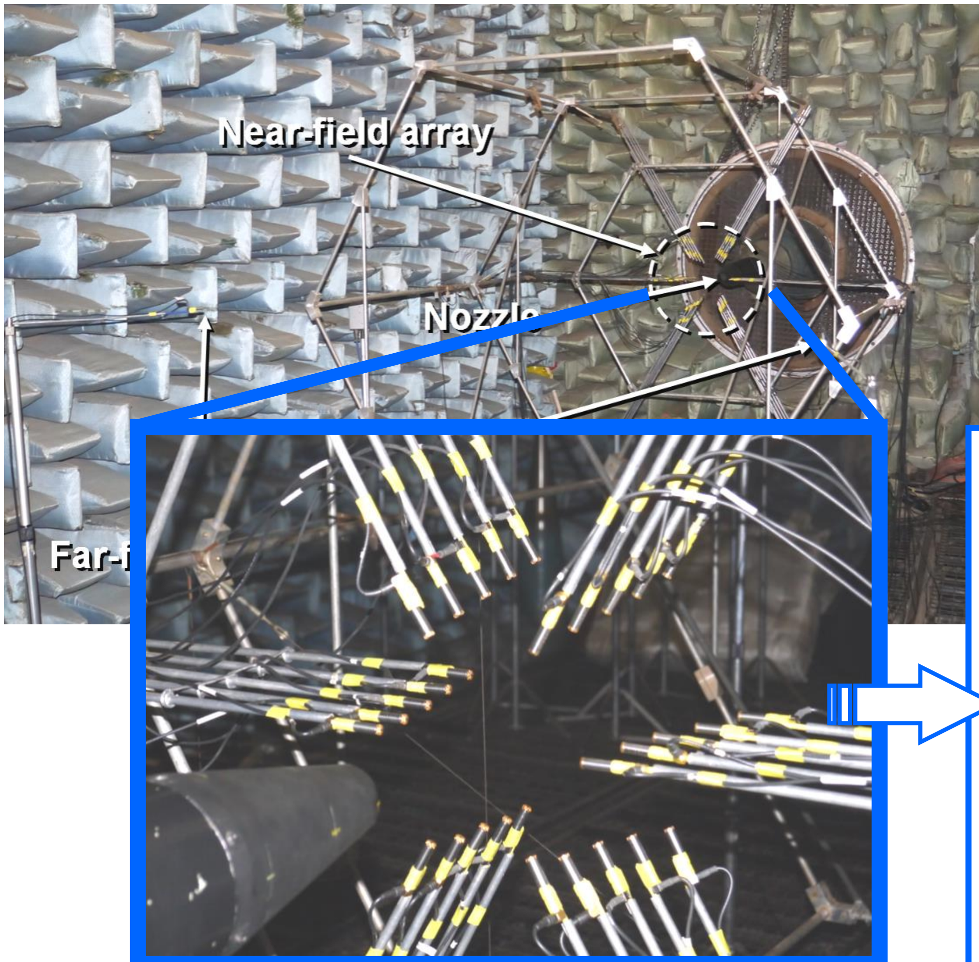

M_j = 0.4, 0.53, 0.6, 0.7, 0.82, 0.88

30 microphones:

- 3 conical surfaces (C1, C2, C3)
- 5 array positions
- x/D=0.5,1.5,…7.5

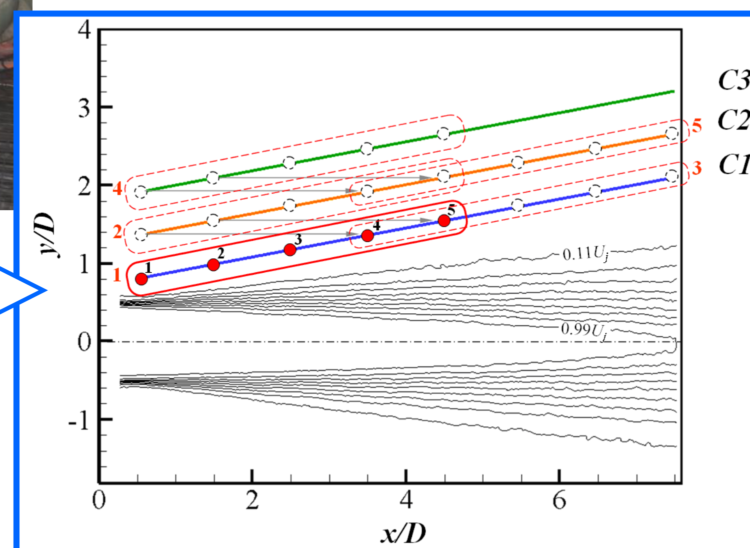

Experimental investigation of the near-field structure

$p(x,R,\theta,t)$ — Raw signals $\xrightarrow{\text{ADT}}$ $A_0(x,R,t)+\sum_{n=1}^{2}\left(A_n(x,R,t)\cos n\theta + B_n(x,R,t)\sin n\theta\right)+A_3(x,R,t)\cos 3\theta+\ldots$ — Azimuthal modes

Raw signals $\xrightarrow{\text{PSD}}$ $p_{total}(x,R,f)$

Azimuthal modes $\xrightarrow{\text{PSD}}$ $a_{0,1,2}(x,R,f)\quad b_{1,2}(x,R,f)$

Typical near-field spectra of the total signal and its azimuthal modes. M_j **= 0.53**

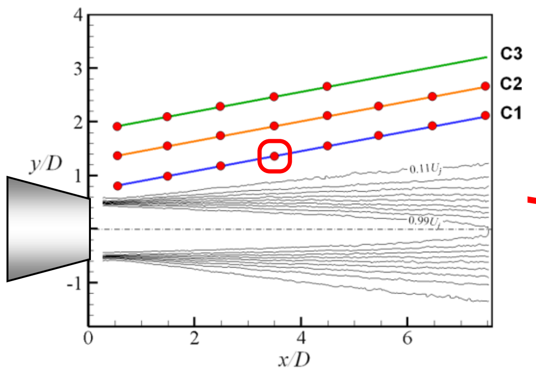

Arndt et al. 1997

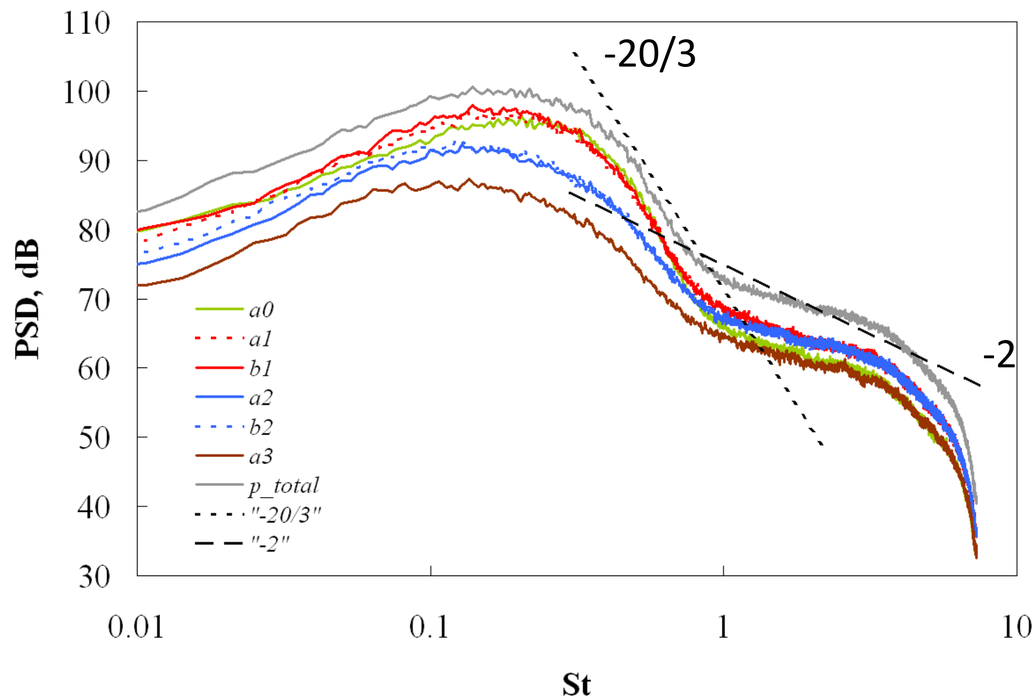

Experimental investigation of the near-field structure

Azimuthal modes M_j=0.4

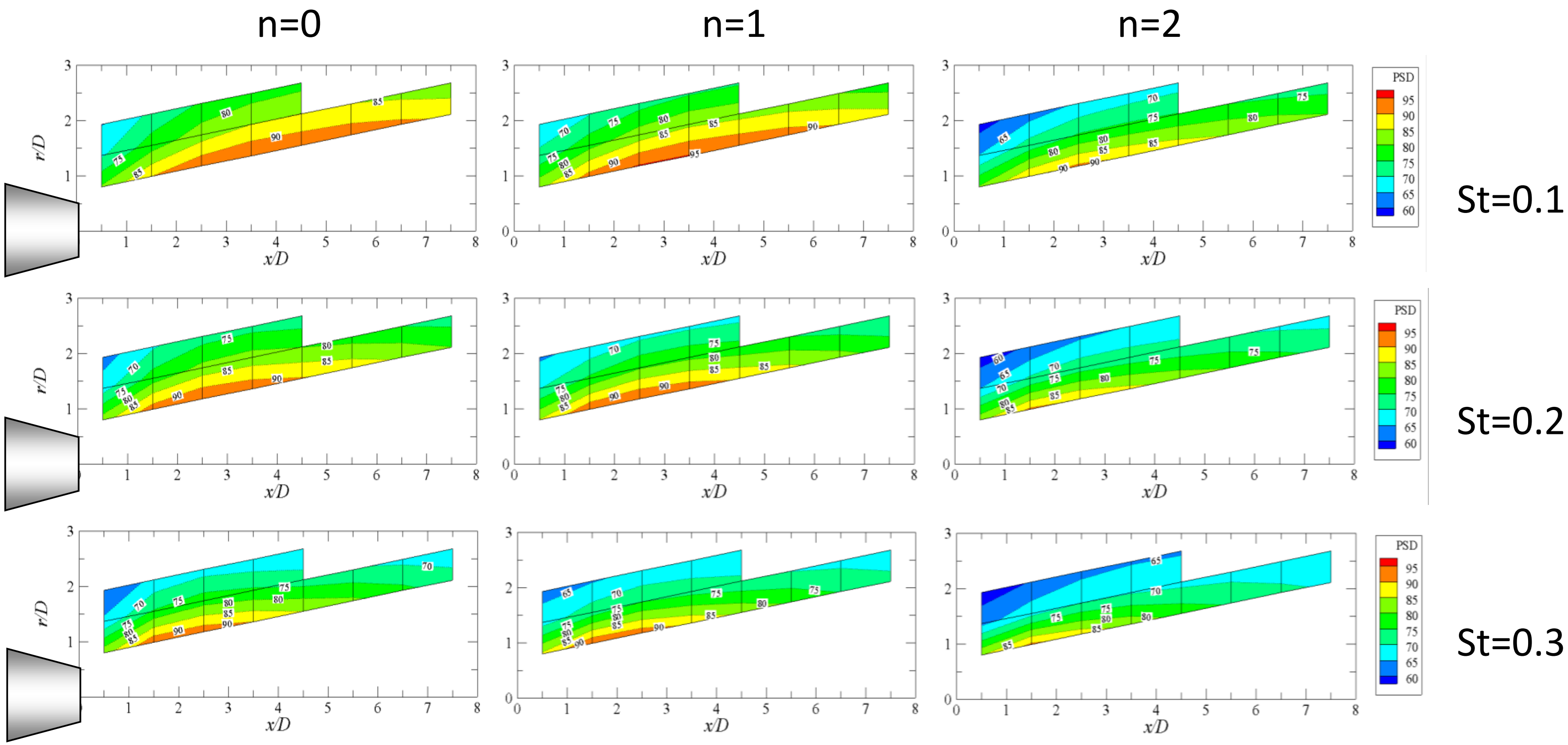

A_n, δ_n, M_n – can be taken from experiments or numerical simulation

Experimental investigation of the near-field structure

Azimuthal modes M_j=0.4

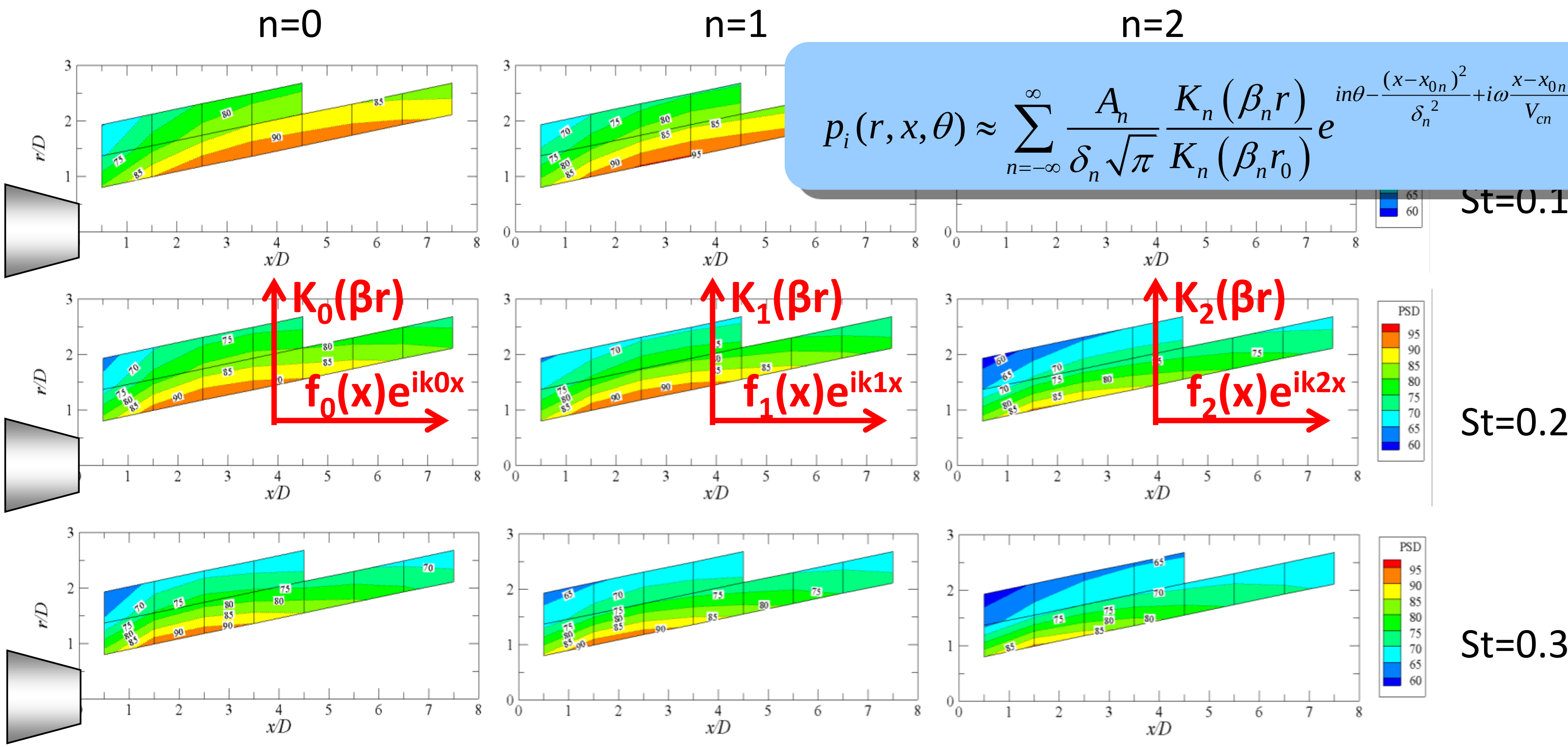

$$p_i(r,x,\theta) \approx \sum_{n=-\infty}^{\infty} \frac{A_n}{\delta_n\sqrt{\pi}} \frac{K_n(\beta_n r)}{K_n(\beta_n r_0)} e^{in\theta - \frac{(x-x_{0n})^2}{\delta_n^2} + i\omega\frac{x-x_{0n}}{V_{cn}}}$$

A_n, δ_n, M_n – can be taken from experiments or numerical simulation

Experimental investigation of the near-field structure

Near-field pressure pulsations on the surface C1 for $M_j = 0.4$

Spatial envelopes | **Relative convection velocities**

mode $n = 0$

mode $n = 1$

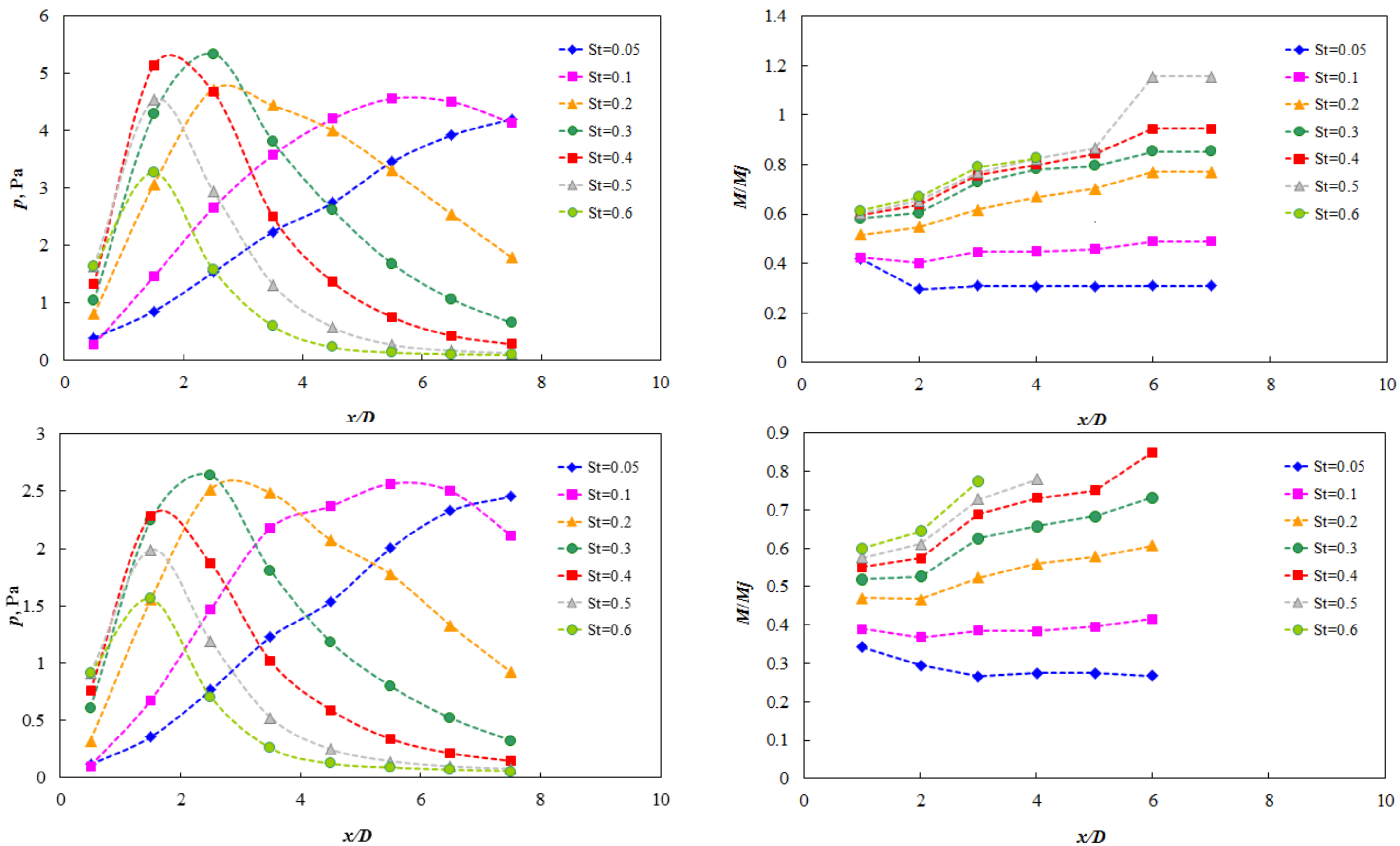

A_n, δ_n, M_n – can be taken from experiments or numerical simulation

Far-field acoustic measurements

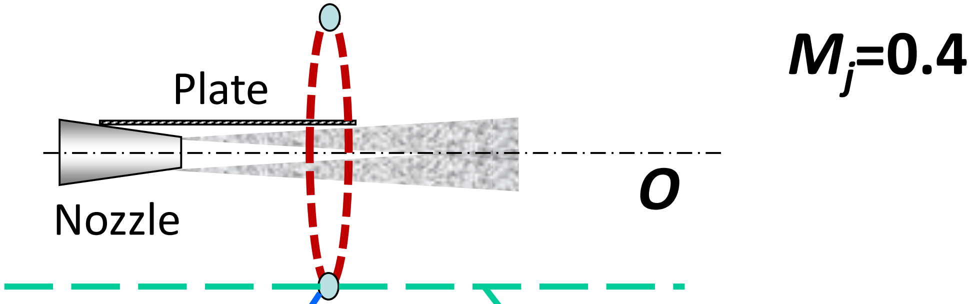

Spectra at sideline direction

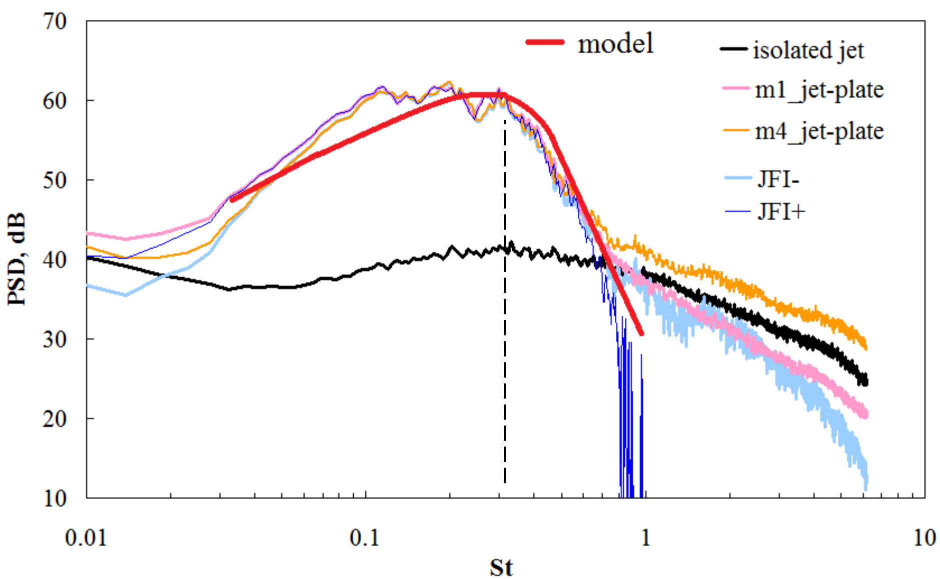

Directivity for St=0.3

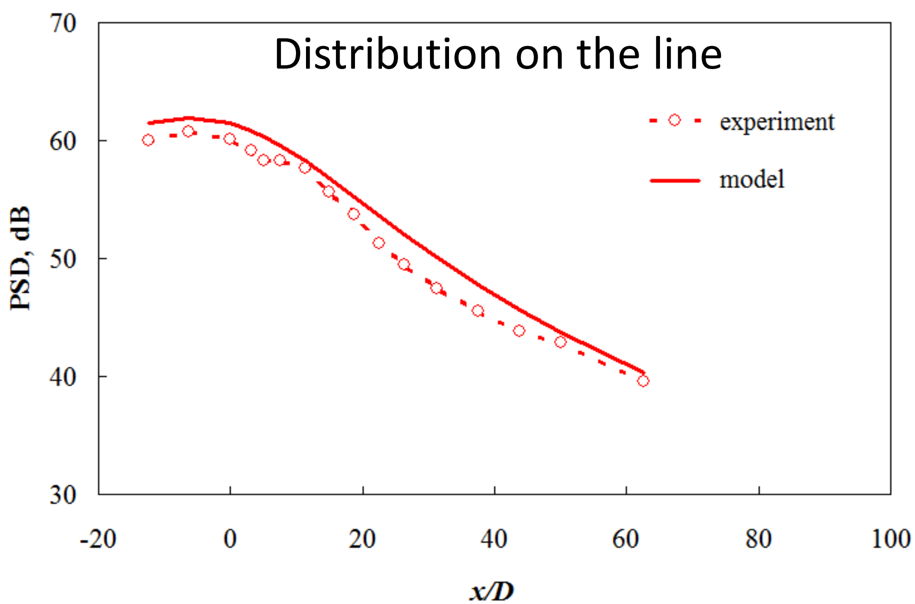

Faranosov et al. (2017, 2018)

Installation noise modeling

Model simplification

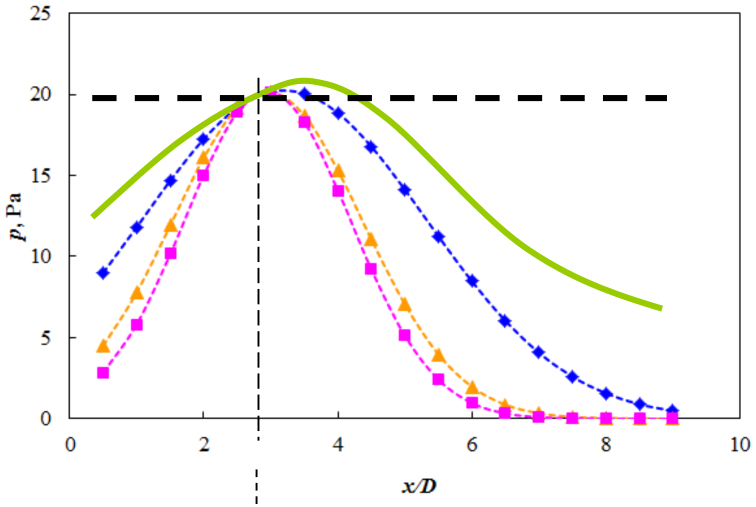

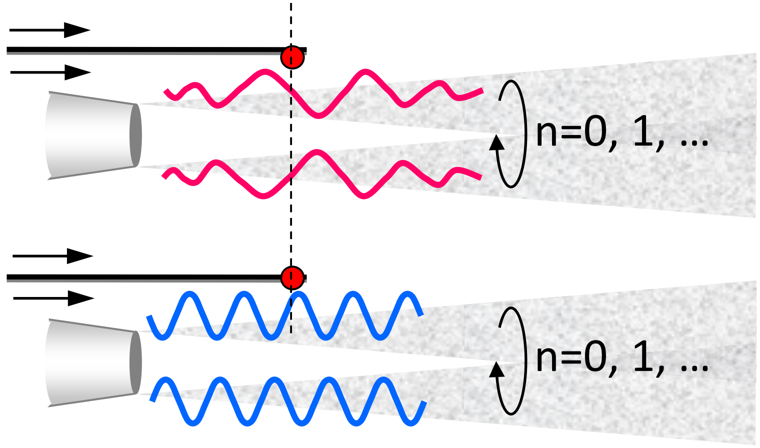

Installation noise modeling

Model simplification

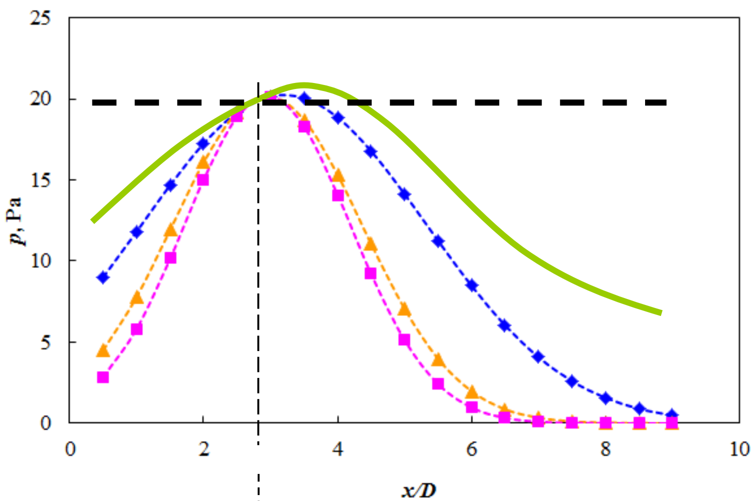

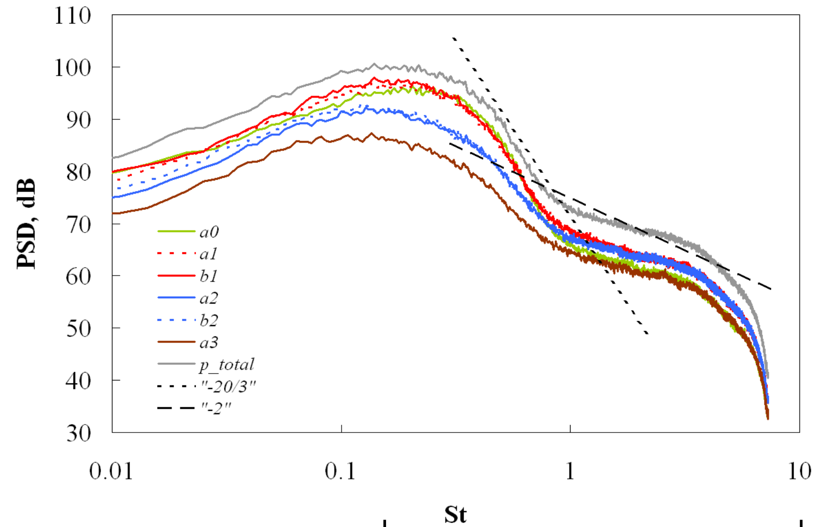

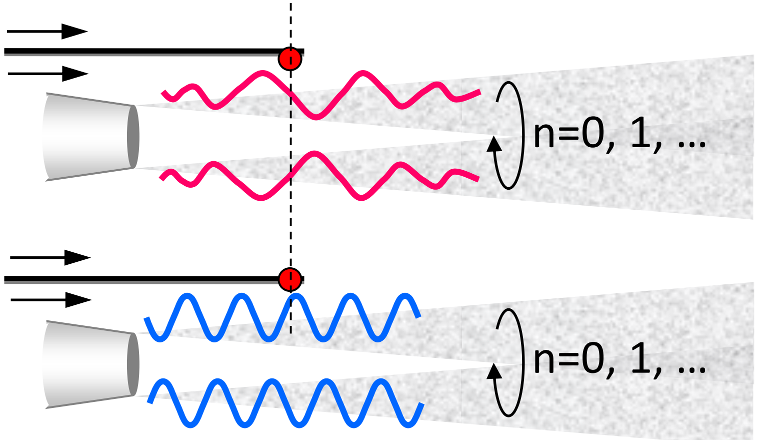

$$\left|p_n(r,\chi)\right| \approx A_n \cdot C_n \left|\frac{\sin(\chi/2)}{\alpha_{sn}\dfrac{M_n}{k} + M_n\cos\chi}\right|$$

Installation noise modeling

Model simplification

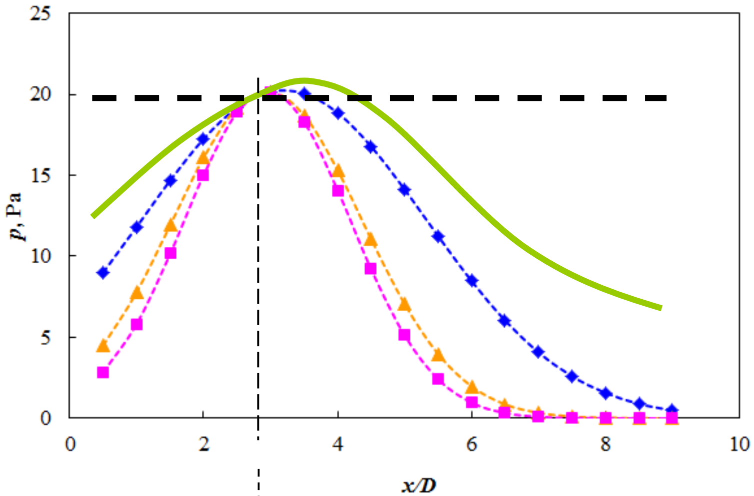

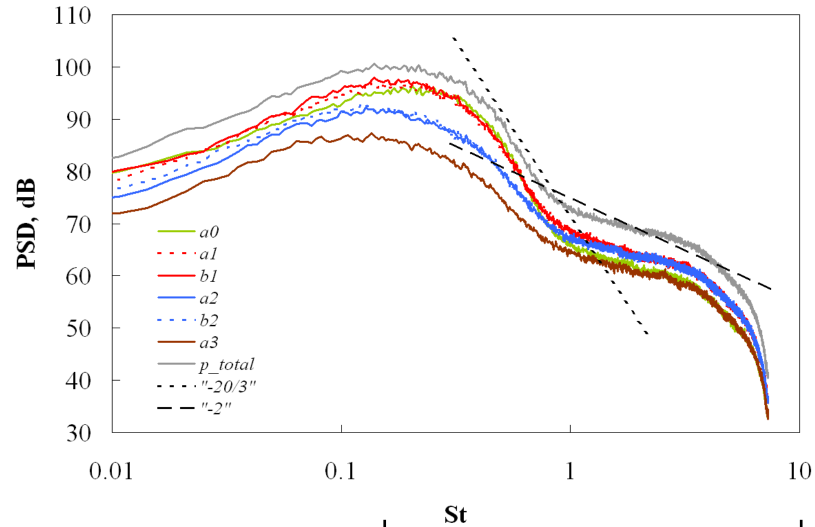

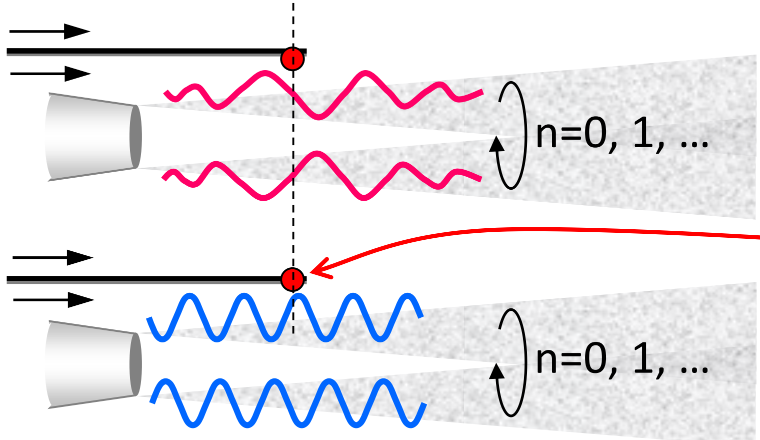

(Dowling et al. 2017)

$$\left|p_n(r,\chi)\right| \approx A_n \cdot C_n \left| \frac{\sin(\chi/2)}{\alpha_{sn}\dfrac{M_n}{k} + M_n \cos\chi} \right|$$

$$p_{total}^2(r,\chi) \approx (A_0^2 + A_1^2) \cdot C_0 \left(\frac{\sin(\chi/2)}{1 - M_0 \cos\chi} \right)^2$$

Outline

- Introduction
- Analytical model description
- Examples of application of the model
  - Jet-plate config. - comparison with experiments
  - Jet-plate config. - comparison with CAA results
  - Jet-wing-flap config. - comparison with experiments
- Conclusion

Numerical simulation of the installed jet

The GPU CABARET solver is used *(Markesteijn et al., 2015)*

Computational domain: 80D x 80D

Grid: 27 mln cells

GPUs: 4 x GTX Titan black

Cold jet, Mj=0.53

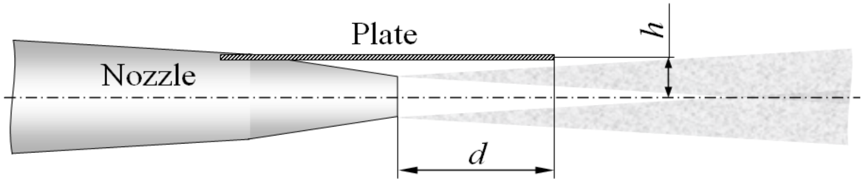

The goal of the simulation is to verify the analytical model.

Low-frequency noise was calculated by three methods:

1. FW-H acoustic analogy

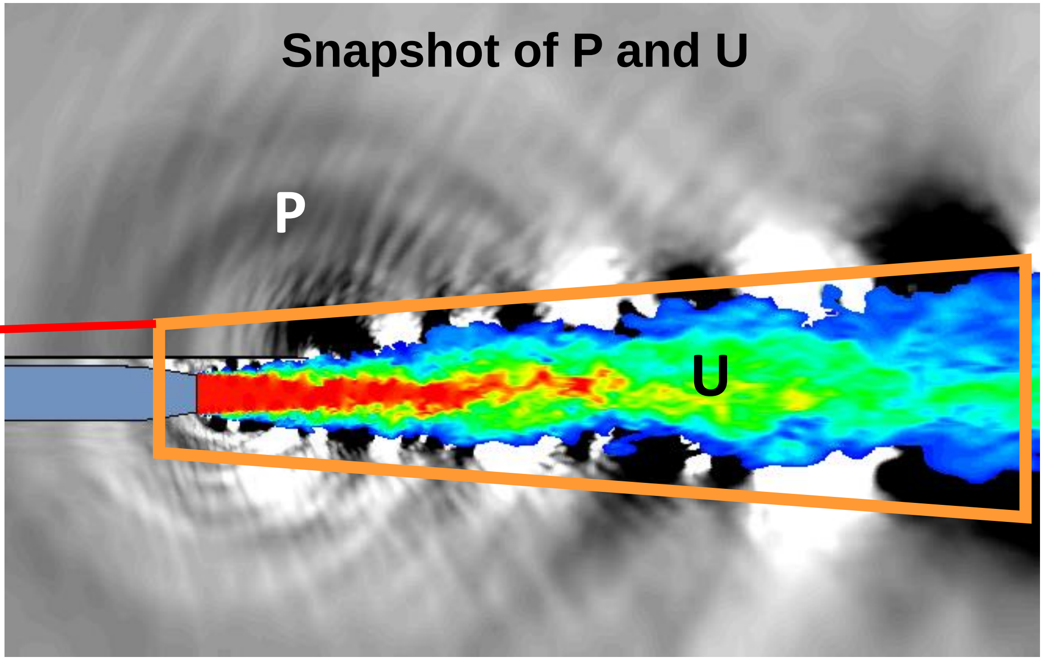

Numerical simulation of the installed jet

The GPU CABARET solver is used *(Markesteijn et al., 2015)*

Computational domain: 80D x 80D

Grid: 27 mln cells

GPUs: 4 x GTX Titan black

Cold jet, Mj=0.53

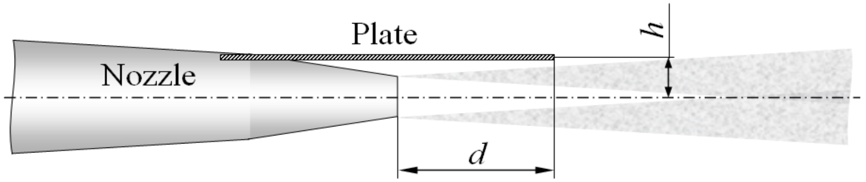

The goal of the simulation is to verify the analytical model.

Low-frequency noise was calculated by three methods:

1. FW-H acoustic analogy

2. On basis of the plate sensors

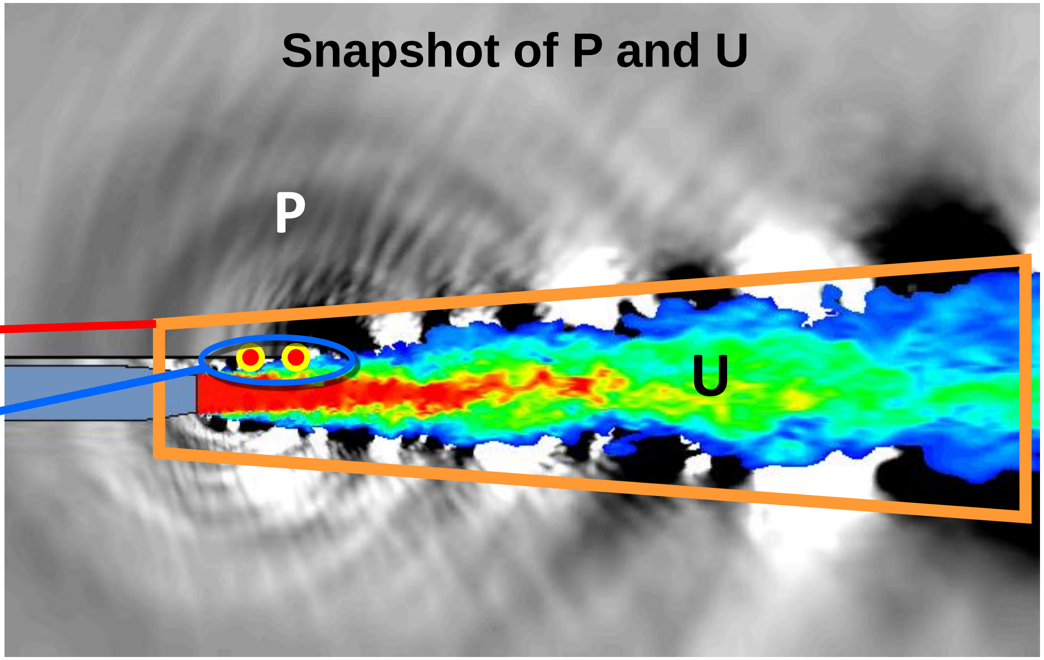

Numerical simulation of the installed jet

The GPU CABARET solver is used *(Markesteijn et al., 2015)*

Computational domain: 80D x 80D

Grid: 27 mln cells

GPUs: 4 x GTX Titan black

Cold jet, Mj=0.53

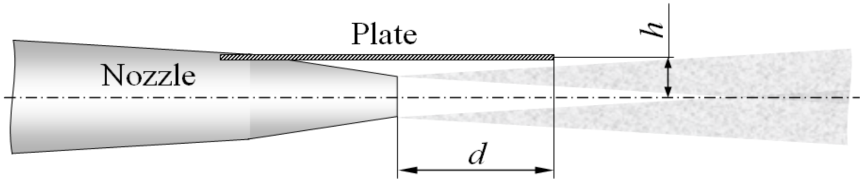

The goal of the simulation is to verify the analytical model.

Low-frequency noise was calculated by three methods:

1. FW-H acoustic analogy
2. On basis of the plate sensors
3. On basis of the free-field sensors

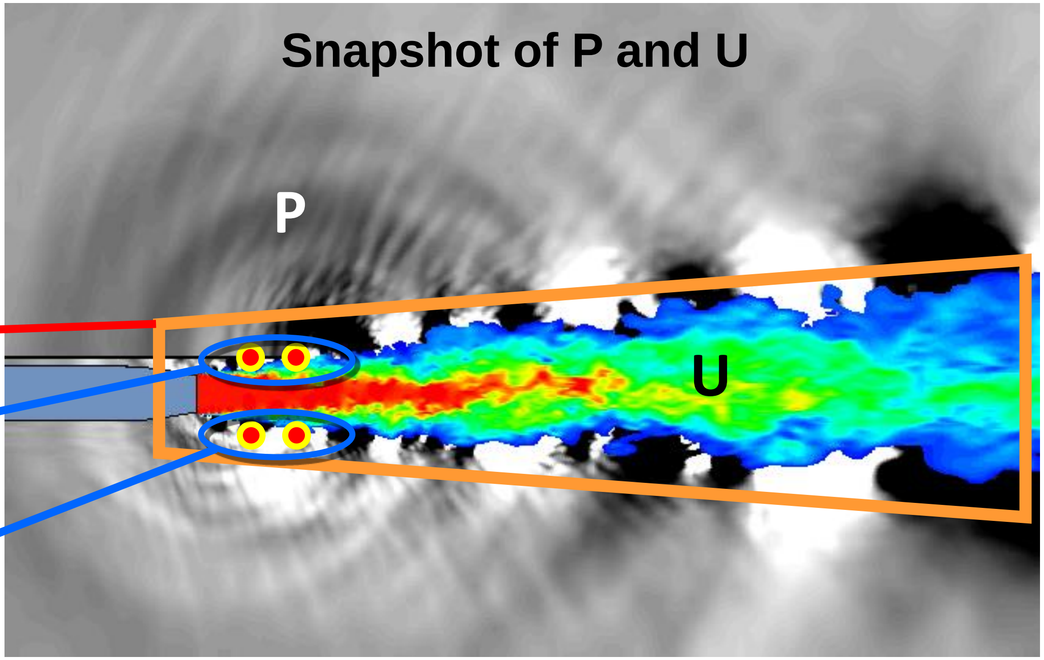

Numerical simulation of the installed jet

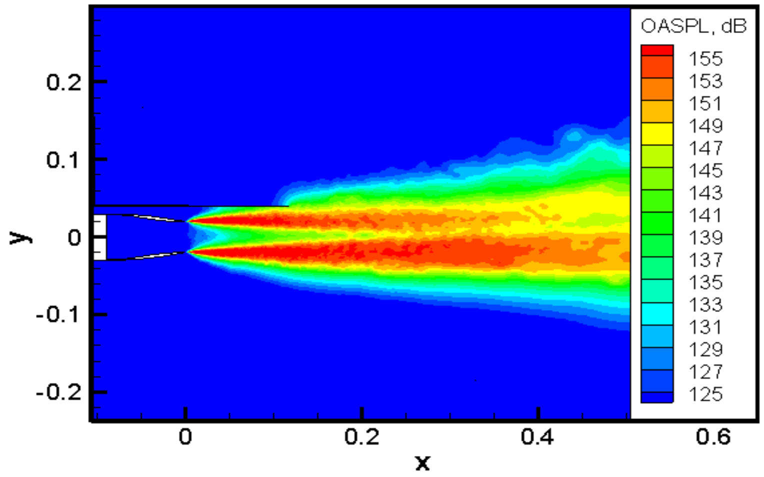

Numerical simulation of the installed jet

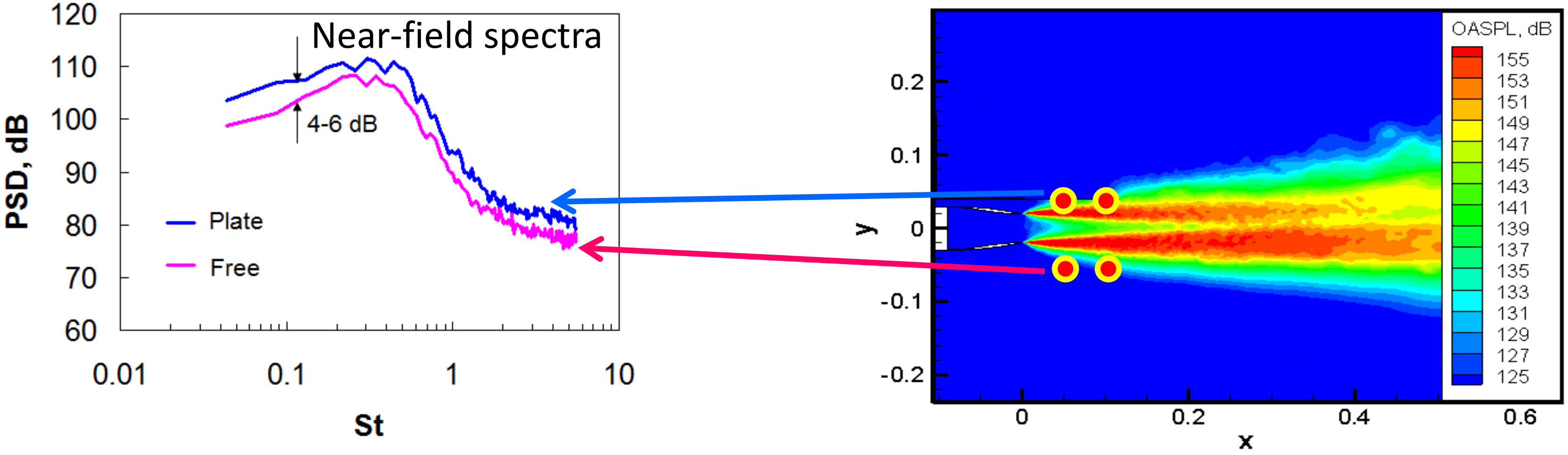

Numerical simulation of the installed jet

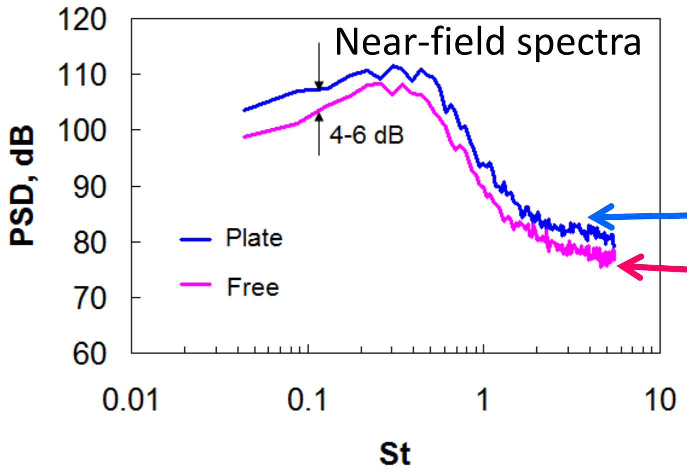

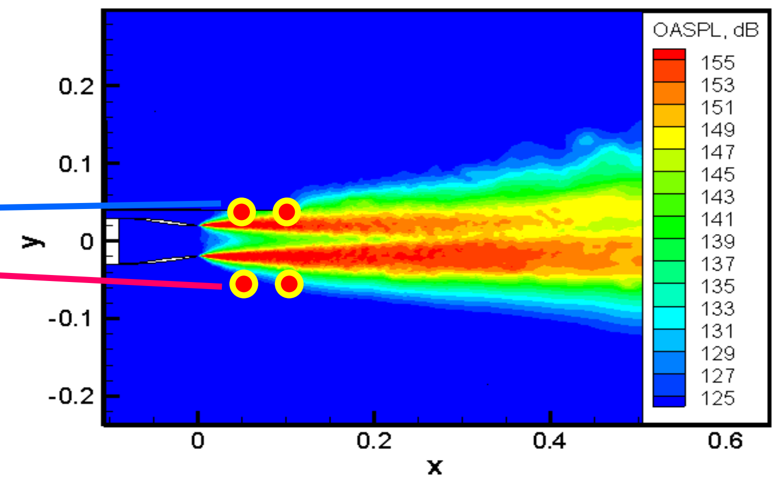

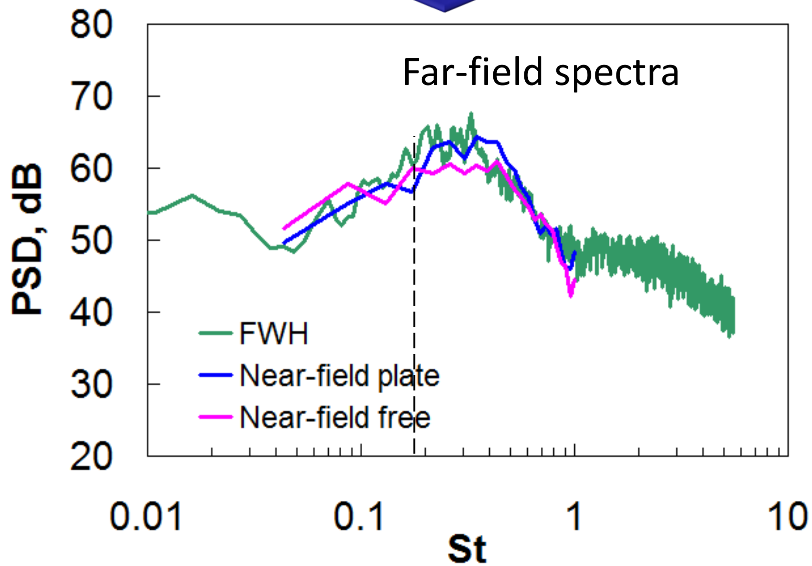

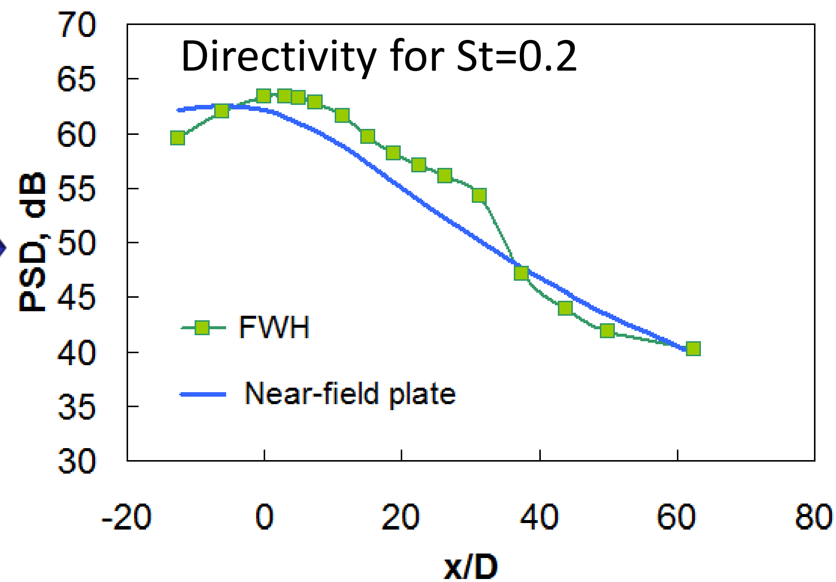

Outline

- Introduction
- Analytical model description
- Examples of application of the model
  - Jet-plate config. - comparison with experiments
  - Jet-plate config. - comparison with CAA results
  - Jet-wing-flap config. - comparison with experiments
- Conclusion

Realistic configuration

Swept wing, flap, double-stream nozzle

Assessment off the pressure pulsations levels on the wing-flap system (2017)

Flush-mounted pressure sensors on the wing

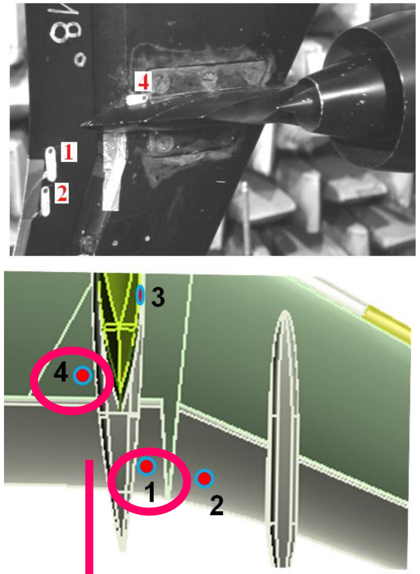

Far-field measurements (Belyaev et al. 2015)

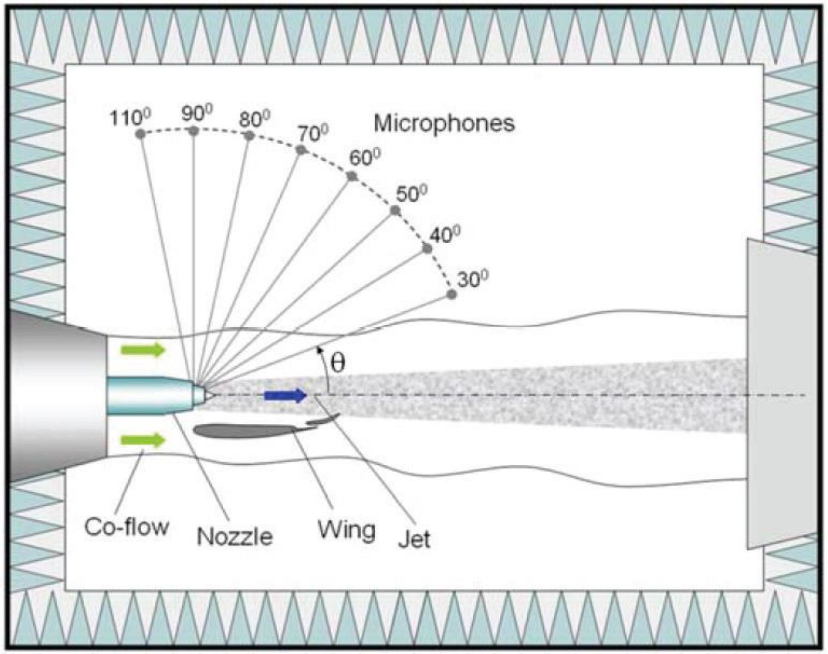

Amplitude and phase speed can be assessed

Realistic configuration

Swept wing, flap, double-stream nozzle

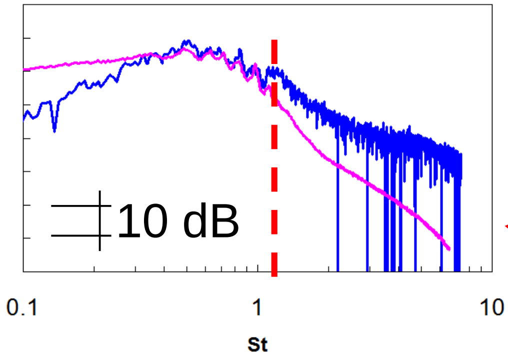

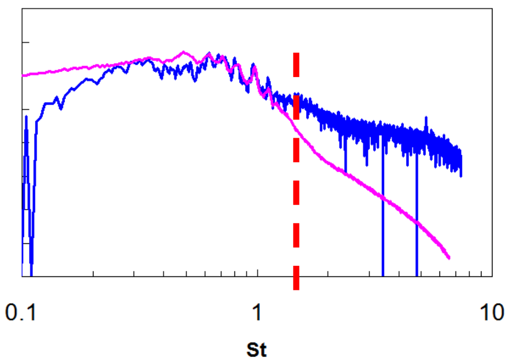

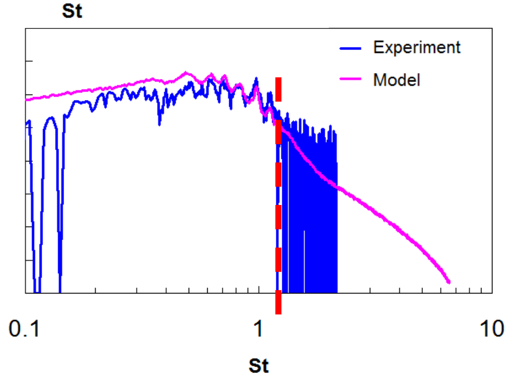

Far-field measurements (Belyaev et al. 2015)

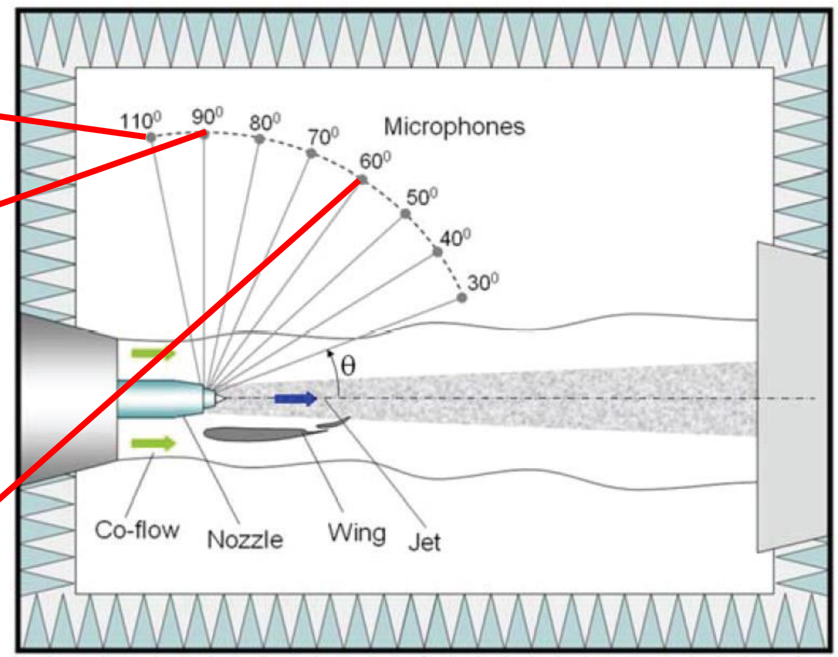

Outline

- Introduction
- Analytical model description
- Examples of application of the model
    - Jet-plate config. - comparison with experiments
    - Jet-plate config. - comparison with CAA results
    - Jet-wing-flap config. - comparison with experiments
- Conclusion

Conclusion

- Robust analytical model of low-frequency jet-wing interaction noise prediction is developed
- The model allows to predict spectral properties and directivity of the installation noise based on the characteristics of the azimuthal modes in the jet near-field
- If the wing is not deeply inserted into the jet shear layer, the model may be simplified so as only the amplitude and phase speed of the total pulsations near the TE are required
- For simplified and realistic configurations, the model gives quite good prediction of the installation noise on basis of the pressure pulsations of the isolated jet as well as pulsations on the wing

Thank you for attention !

Jet noise modeling

L_{jet} is represented in terms of superposition of quadrupole-type sources *(Kopiev&Chernyshev, 2012)*.

The sources are assumed to be compact and possess certain stochastic properties (*Tam&Auriault, 1999*) dictated by experimental results.

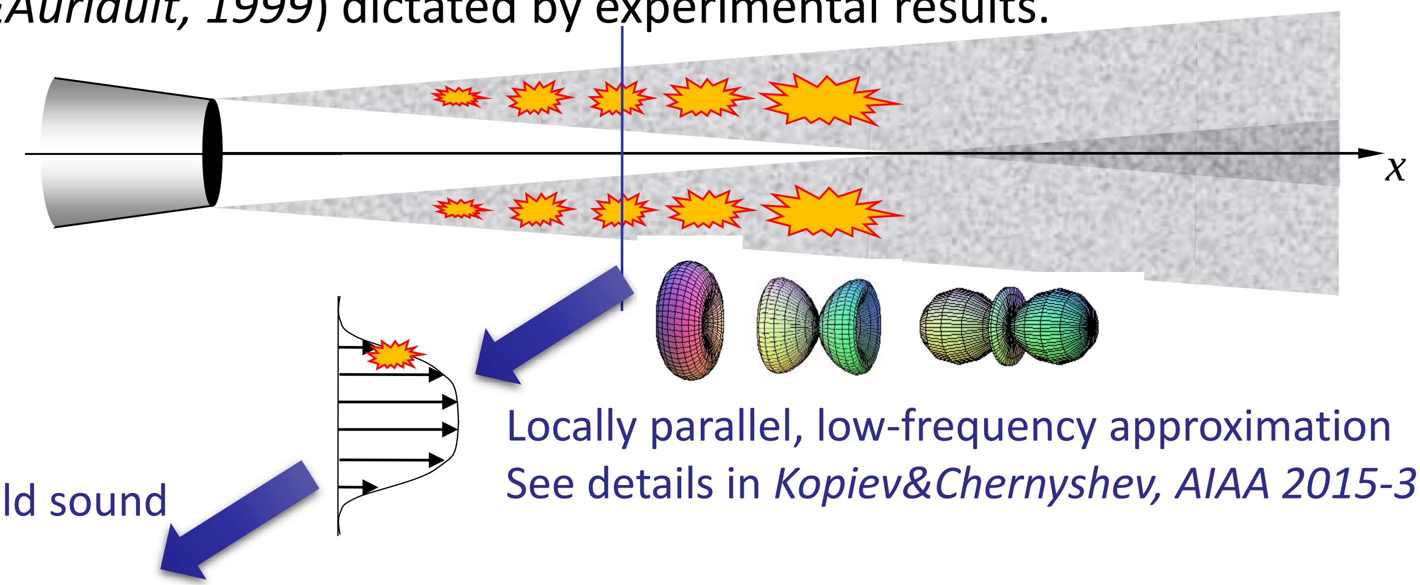

$$\Phi_{p[m]}(R,x,\omega) \approx \sum_{n=1}^{6} \int \left| I_{n[m]}(R,x,x',\omega) \right|^2 \frac{l^3}{\sqrt{2\pi}} A_n(x',\omega)\,dx'$$

$$\tau_0\big|_{V_{jet}} = \frac{120}{V_{jet}} \tau_0\big|_{V=120}$$

$$I_{n[m]}(R,x,x',\omega) = \frac{2}{|\mathbf{r}-\mathbf{r}'|} \frac{F_{n[m]}(\alpha,\omega)}{\left[1-i(\omega-\alpha U)\tau_0\right]} \exp\left(ik|\mathbf{r}-\mathbf{r}'| - i\frac{m\pi}{2} - i\frac{\pi}{2} \right)$$

$$A\big|_{V_{jet}} = \left(\frac{V_{jet}}{120} \right)^n A\big|_{V=120}$$

Installation noise modeling

L_{inst} is modeled on basis of the approach proposed in *Bychkov et al. AIAA 2016-2932*.

It is assumed that the near-field of the isolated jet can be considered as incident field on the plate, near-field pulsations are assumed to obey wave equation.

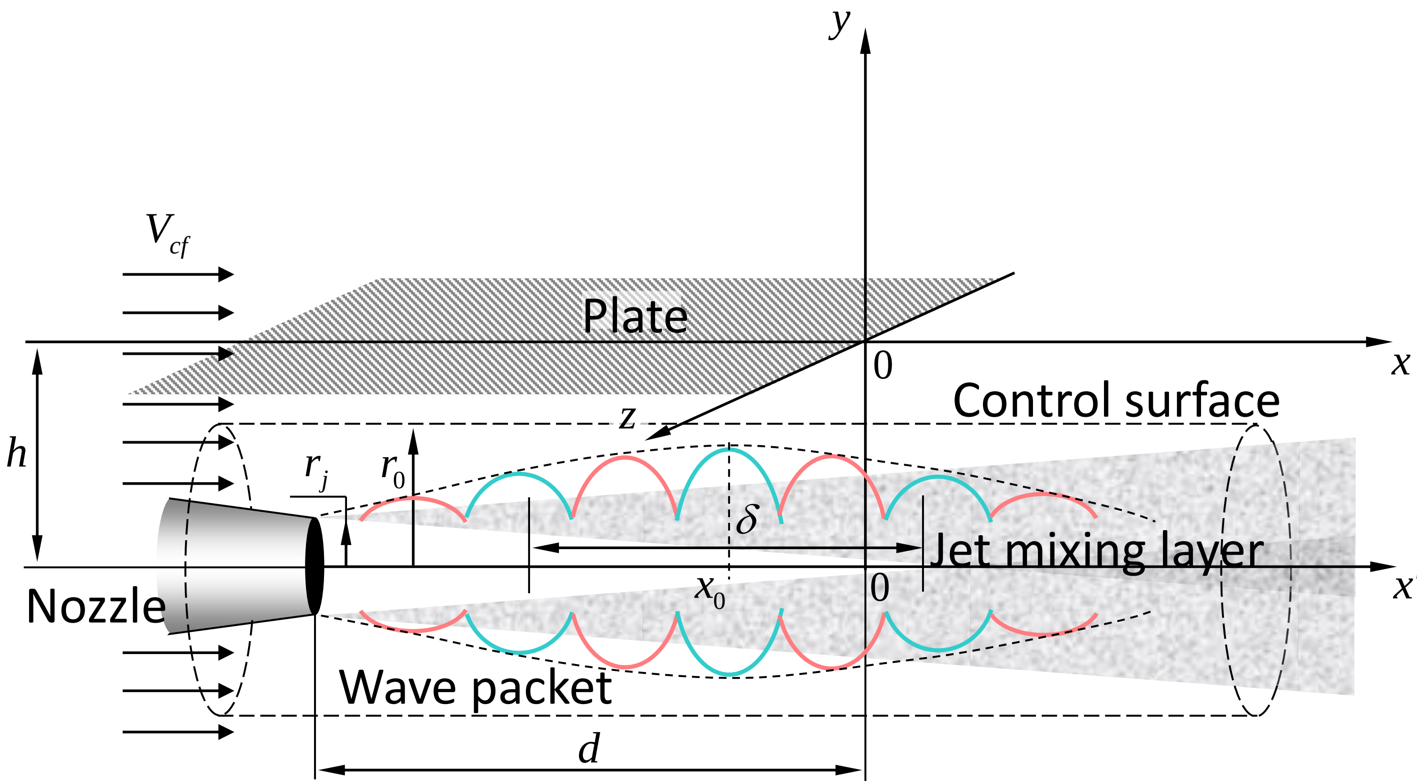

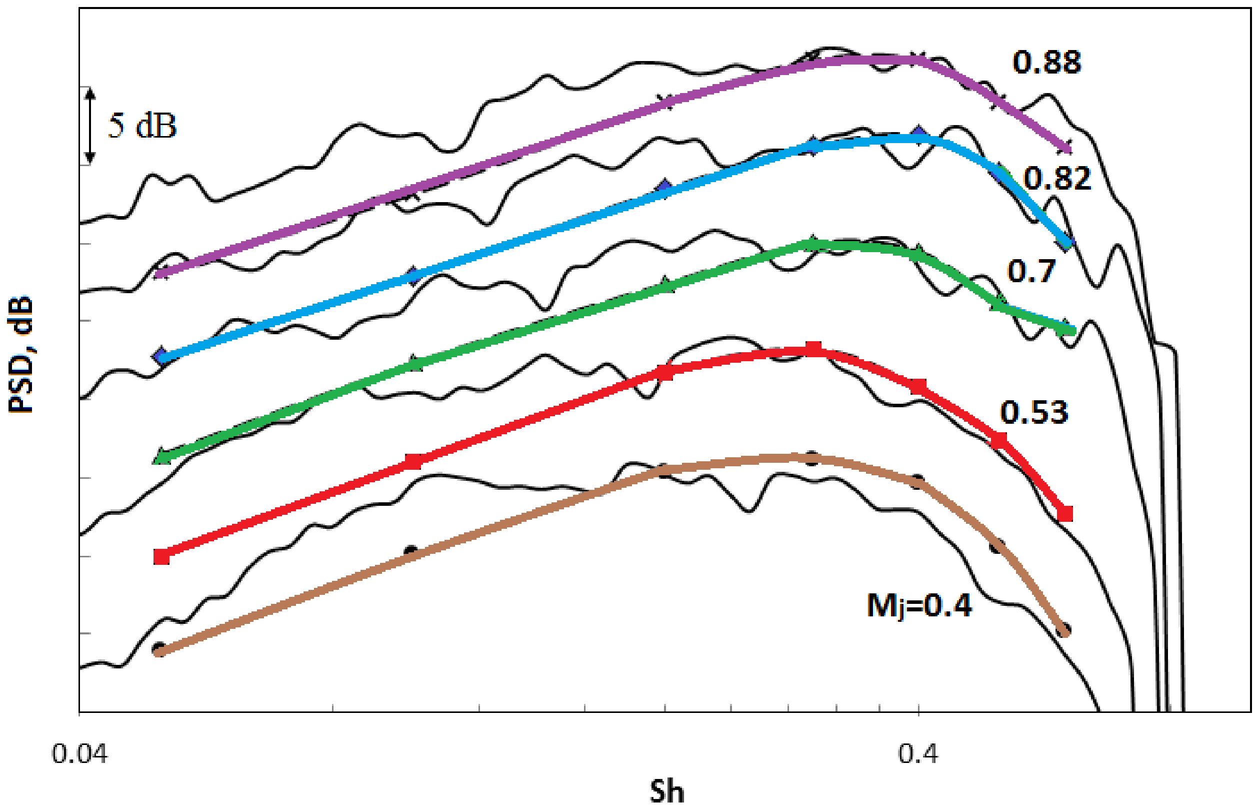
0.88
5 dB
0.82
0.7
0.53
Mj=0.4
PSD, dB
0.04
0.4
Sh

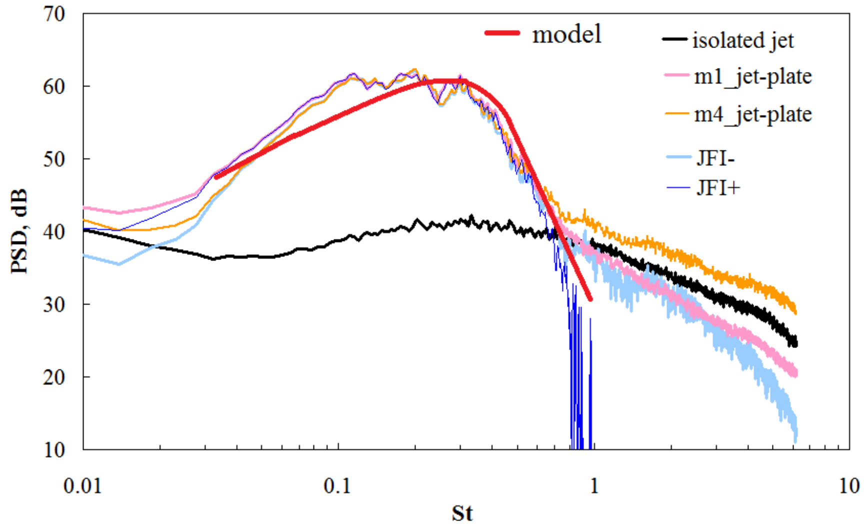

70
60
50
40
30
20
10
PSD, dB
model
isolated jet
m1_jet-plate
m4_jet-plate
JFI-
JFI+
0.01
0.1
1
10
St

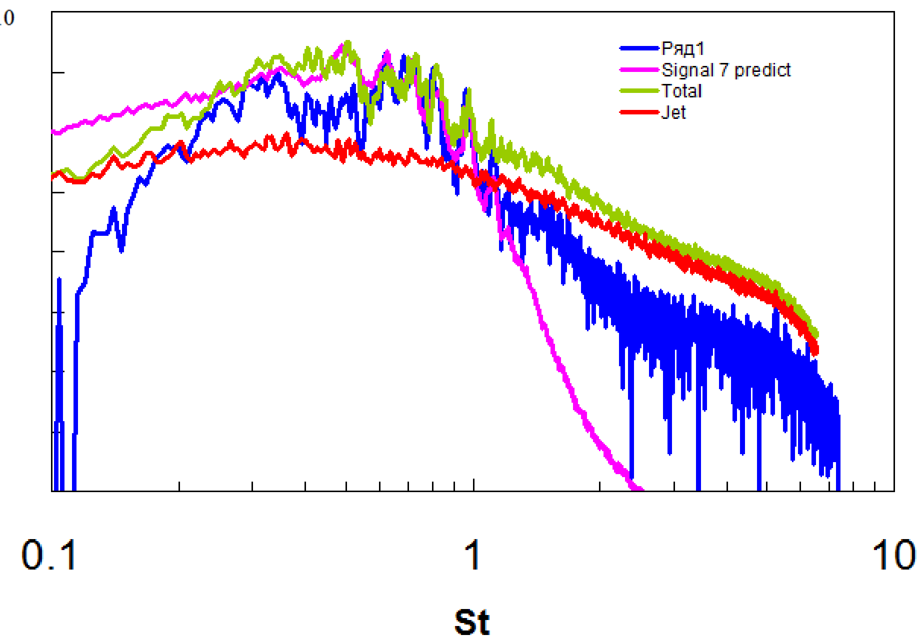

Ряд1
Signal 7 predict
Total
Jet
0.1
1
10
St